

Image Cover Sheet

CLASSIFICATION

UNCLASSIFIED

SYSTEM NUMBER

121964



TITLE

A REVIEW OF HYDRODYNAMIC ADDED MASS INERTIA OF VIBRATING SUBMERGED
STRUCTURES

System Number:

Patron Number:

Requester:

Notes:

DSIS Use only:

Deliver to: JR





National Defence
Research and
Development Branch

Défense Nationale
Bureau de Recherche
et Développement

TECHNICAL MEMORANDUM 84/F

April 1984

**A REVIEW OF
HYDRODYNAMIC ADDED MASS INERTIA
OF
VIBRATING SUBMERGED STRUCTURES**

J. E. Slater

**UNLIMITED
DISTRIBUTION
ILLIMITÉE**

**Defence
Research
Establishment
Atlantic**



**Centre de
Recherches pour la
Défense
Atlantique**

Canada



National Defence
Research and
Development Branch

Défense Nationale
Bureau de Recherche
et Développement

A REVIEW OF
HYDRODYNAMIC ADDED MASS INERTIA
OF
VIBRATING SUBMERGED STRUCTURES

J. E. Slater

April 1984

Approved by T. Garrett

Director / Underwater Acoustics Division

DISTRIBUTION APPROVED BY

CHIEF D. R. E. A.

TECHNICAL MEMORANDUM 84/F

Defence
Research
Establishment
Atlantic



Centre de
Recherches pour la
Défense
Atlantique

Canada

ABSTRACT

This report is a review of the methods developed for predicting the hydrodynamic added mass inertia of vibrating structures floating or submerged in a fluid. The fluid surrounding a vibrating structure causes an apparent increase in the mass inertia of the structure, which substantially reduces the natural resonant frequencies and alters the dynamic response.

The various methods consist of the three basic approaches; analytical, empirical and numerical. This report presents the merits and limitations of the methods by indicating their suitability to predict the added mass inertia effects of structures such as plates, foils, marine propellers and ship hulls.

No one universal method has been developed to satisfactorily predict the added mass effects, but a variety of methods can be used to handle many configurations of interest. For detailed analysis, the numerical finite element methods are vastly superior. Nonetheless, for conceptual and preliminary design analyses, simpler methods using analytical and empirical formulas may be sufficiently accurate besides being faster and cheaper to use than finite element modeling of the fluid. However, some of these methods are applicable only to 2-D or axisymmetric structures as well as being restricted to essentially the zero frequency limit.

RESUME

Le présent rapport traite des méthodes de prévision de l'inertie de masse hydrodynamique ajoutée des ouvrages vibrants qui flottent ou qui sont immergés dans un fluide. Le fluide autour d'un ouvrage vibrant donne lieu à une augmentation apparente de l'inertie de l'ouvrage, à une réduction importante des fréquences naturelles de résonance et à une modification de la réponse dynamique.

Les différentes méthodes consistent en trois approches de base: analytique, empirique et numérique. Le présent rapport décrit les mérites et les limites des méthodes en indiquant si elles conviennent à la prévision de l'augmentation de l'inertie d'ouvrages tels que plaques, feuilles métalliques, hélices et coques de bateaux.

Aucune méthode universelle n'a été mise au point pour prévoir les effets de masse ajoutée, mais diverses méthodes peuvent être utilisées pour un grand nombre de configurations d'intérêt. Pour une analyse détaillée, les méthodes numériques par éléments finis sont de loin les meilleures. Néanmoins, pour des analyses conceptuelles et préliminaires, des méthodes plus simples faisant intervenir des formules analytiques et empiriques peuvent être suffisamment précises sans compter qu'elles sont plus rapides et coûtent moins cher que la modélisation par éléments finis du fluide. Cependant, certaines de ces méthodes ne valent que pour des ouvrages bidimensionnels ou axisymétriques et sont essentiellement limitées à la limite de fréquence nulle.

TABLE OF CONTENTS

	<u>Page No.</u>
ABSTRACT	ii
NOTATION	v
1. INTRODUCTION	1
2. THEORETICAL BACKGROUND	1
2.1 Equations of Motion	2
2.2 Hydrodynamic Added Mass	4
3. PREDICTIVE TECHNIQUES	5
3.1 Analytical Methods	5
3.2 Empirical Methods	6
3.3 Numerical Methods	7
4. DISCUSSION	8
4.1 Two and Three Dimensional Rigid Bodies	9
4.2 Plates and Foils	10
4.3 Marine Propellers	11
4.3.1 Complete Propeller	12
4.3.2 Propeller Blade	14
4.3.3 Summary of Methods for Propellers	16
4.4 Cylinders and Ship Hulls	16
4.4.1 Empirical Methods	16
4.4.2 Potential Flow Methods	19
4.4.3 Finite Element Methods	20
4.4.4 Summary of Methods for Cylinders and Ship Hulls	22
5. CONCLUDING REMARKS	23
TABLES	24
FIGURES	44
REFERENCES	66
DOCUMENT CONTROL DATA	67

NOTATION

a	characteristic dimension of acoustic radiating body (e.g. piston radius).
B	ship hull breadth at section waterline
B.A.R.	blade area ratio for propeller
[C]	damping coefficient
C	Lewis hull form section coefficient
c	speed of sound in the fluid
[D]	acoustic energy radiation dissipative boundary condition
D	propeller diameter
D	cantilever plate stiffness coefficient = $Eh^3/12(1-\nu^2)$
E	Young's modulus of elasticity
f_a	natural resonant frequency in air
f_w	natural resonant frequency in water
$f(t)$	time varying forces
g	acceleration of gravity
[H]	matrix of Laplace operator $\nabla^2 = \partial^2/\partial x^2 + \partial^2/\partial y^2 + \partial^2/\partial z^2$
h	water depth
I_A, I_h	hydrodynamic added polar mass moment of inertia for propeller
I_p, I_b	polar mass moment of inertia for propeller structure
I_w	polar mass moment of inertia of the "equivalent-water" propeller
J	advance ratio for propeller = advance speed/ND
J	longitudinal reduction factor for ship hulls

[K]	structural stiffness
K_A	added mass correction factor or coefficient for translational motion
K_I	added inertia correction factor or coefficient for rotational motion
k	underwater acoustic wave number = $2\pi/\lambda = \omega/c$
ka	frequency parameter
[L]	coupling interactive loading parameter
[M]	structural mass
$[M_A], M_A$	predicted hydrodynamic added mass inertia
M_A	Lewis hull form hydrodynamic added mass per unit length
M_A	hydrodynamic added mass of a propeller with unrestrained shaft rotation
m_A	actual hydrodynamic added mass inertia
M_p	mass of propeller
MWR	mean width ratio of marine propeller
N	propeller revolutions per second
n	number of propeller blades
P	nominal propeller pitch
p	fluid pressure
$[\bar{Q}]$	parameter $\bar{Q} = Q + Q_0$
Q	compressibility term of the Helmholtz equation
Q_0	surface wave parameter
T	ship hull draft
X_M	imaginary reactive component of acoustic radiation impedance = $2\pi f_w M_A$

β	Lewis hull form sectional area coefficient $\beta = \text{section area}/(\text{breadth} \times \text{draft})$
δ	generalized structural displacement
$\theta_{2/3}$	pitch angle of propeller blade for section at 2/3 full radius
λ	acoustic wave length in water
λ	wave length of mechanical vibration
ν	structural frequency wave number = ω^2/g
ν	Poisson's ratio
ρ	fluid density
ρ_p	plate material density
ω, ω_n	circular frequency (radians/sec)
.	differentiation with respect to time
{ }	vector
[]	matrix
[] ^T	matrix transpose
[] ⁻¹	matrix inverse

1. INTRODUCTION

The vibration of a submerged structure induces motion in the surrounding fluid which causes an apparent increase in the mass inertia of the structure. This increase in mass is known as the hydrodynamic added mass inertia. In the field of naval architecture, the most important problems involving the effects of the mass inertia are concerned with rigid body ship motions, fluid storage and conveyance, and elastic vibration of hull main structure and associated appendages such as propellers, rudders and various hydrodynamic control and lifting surfaces. Experimental measurements of the added mass inertia have been performed using full scale and model structures with some success. Because these measurements are expensive and time consuming, attempts have been made to develop methods which reliably predict the magnitude of the added mass inertia effect.

This technical memorandum is a review of the methods developed for the prediction of the hydrodynamic added mass inertia of vibrating submerged structures. It considers three basic approaches 1) analytical, 2) empirical and 3) numerical, and discusses their merits and limitations. The report indicates the suitability of the methods to predict the added mass inertia of structures such as plates and foils, marine propellers and ship hulls. The tables and figures presented in this report have been extracted from the referenced literature to illustrate and compare the results of the various methods. As this information was taken from the work of different authors, there is some variation in the presentation and notation of the results.

2. THEORETICAL BACKGROUND

The hydrodynamic added mass inertia can substantially reduce the natural resonant frequencies and alter the dynamic response of a vibrating submerged structure. The resulting effects depend on the shape and size of the structure, material to fluid density ratio, vibratory mode shape and frequency as well as the type and extent of the fluid boundaries. Observations indicate that the fluid inertia has a greater effect on the lower elastic modes since the fluid moves mainly in the direction of body motion. Also, confinement of the fluid in a rigid channel has a tendency to increase the hydrodynamic mass; whilst placing the structure near an air-water interface or other pressure release boundary decreases the hydrodynamic mass effect.

The technical literature on the interaction of a vibrating structure with a surrounding fluid can be traced back to the original works of Stokes¹, Lamb² and Rayleigh³. Since then, much has been written in the literature on this subject⁴⁻¹⁹ either dealing directly with the evaluation of hydrodynamic added mass inertia or the development of techniques to solve the complete fluid-structure interaction problem in which case added mass is but one of many parameters that has to be determined. The analytical methods discussed in this technical memorandum will be limited to the evaluation of added mass.

2.1 Equations of Motion

The basic theory for the coupled motion of an elastic structure in a fluid has been given by Zienkiewicz^{20,21} and Kalinowski⁵. The general equations of motion for the structure and fluid are as follows:

$$[M]\{\ddot{\delta}\} + [C]\{\dot{\delta}\} + [K]\{\delta\} = \{f(t)\} + \text{Hydrodynamic Forces} \quad (1)$$

$$[\bar{Q}]\{\ddot{p}\} + [D]\{\dot{p}\} + [H]\{p\} = \text{Interface Pressure Loading} \quad (2)$$

In equation (1) for the structure, M, C and K are the mass, damping and stiffness; δ is a generalized displacement, and $f(t)$ are the time varying applied forces except for those of hydrodynamic origin, which are indicated separately. The damping parameter includes the linear viscous effects of the fluid. The generalized displacements and hydrodynamic forces have six components related to the three translational and three rotational degrees of freedom.

Equation (2) for the fluid has been determined from the basic Navier-Stokes equation of fluid motion with the assumption that the second order convective acceleration terms are small and can be omitted. In addition, the non-linear terms associated with viscosity are neglected so that the viscous effects reduce to the linear viscous damping model proportional to the body velocity and are incorporated in the damping parameter C (equation (1)). Therefore, the fluid, described by equation (2), is considered to be inviscid.

In equation(2), matrix H contains the Laplace operator representing the second derivatives with respect to the three coordinate variables. The compressibility of the fluid appears in the first two terms of the fluid equation. $\bar{Q} = Q + Q_0$, where Q is the compressibility term from the Helmholtz wave equation associated with the second time derivative of the fluid pressure, p. In the second term of equation (2), D represents the acoustic energy propagating away from the moving body. For mathematical representation, the infinite expanse of fluid is truncated at a 'sufficiently large' distance, typically one to four times the body dimension, to have negligible effect on the accuracy of the solution. The acoustic energy radiation parameter D implies a dissipative boundary condition such that energy is only radiated away from the body and not reflected back. To simplify the analysis of fluid-structure interaction, incompressibility of the fluid is assumed. Thus, the terms associated with Q and D drop out. Generally, this has little appreciable effect on the validity of the solution.

In addition to the hydrodynamic added mass, the effects of the fluid inertia may occur in the form of gravity surface waves represented by the linearized free-surface boundary condition parameter Q_0 . The gravity waves are produced by vibrating bodies that are either floating or sufficiently close to the surface. In many cases, however, for elastic vibration of large structures such as ship hulls and completely immersed appendages like propeller blades and stabilizer fins, the surface waves have little affect and may be neglected to simplify the mathematical analysis.

Zienkiewicz revealed that the coupling between the motion of the structure and the fluid occurs via their interface surfaces through the hydrodynamic forces and interface pressure loading terms in equations (1) and (2). To relate these two terms, a coupling interactive loading matrix [L] is derived in the form of shape functions which describe the structural normal displacement pattern and the resultant fluid pressure distribution over the interface surfaces.

By introducing matrix [L] and assuming the fluid medium is incompressible and free of surface waves, the governing equations (1) and (2) become

$$[M]\{\ddot{\delta}\} + [C]\{\dot{\delta}\} + [K]\{\delta\} = \{f(t)\} + [L]\{p\} \quad (3)$$

$$[H]\{p\} = -\rho[L]^T\{\ddot{\delta}\} \quad (4)$$

By inverting matrix [H] and substituting {p} into equation (3), the equation for the structure can be rearranged to the form

$$([M] + \rho[L] [H]^{-1}[L]^T) \{\ddot{\delta}\} + [C]\{\dot{\delta}\} + [K]\{\delta\} = \{f(t)\} \quad (5)$$

Thus for the vibrational analysis of a submerged structure when neglecting compressibility and surface wave effects, the governing equation is of standard form except for the additional mass term

$$[M_A] = \rho[L] [H]^{-1} [L]^T \quad (6)$$

M_A is referred to as the hydrodynamic added mass.

2.2 Hydrodynamic Added Mass

As shown by equation (6), the hydrodynamic added mass is dependent upon the interactive matrix [L], which contains the shape functions for the interface surface displacements and pressures. This suggests that the added mass is inherently dependent on the structural vibrational mode shape and frequency. This is analogous to the fundamental principle in the field of underwater acoustics, where it is known that the acoustic radiation impedance of a body depends on the relationship of the body shape, surface displacement and acoustic wavelength to body size.^{22,23}

To develop an understanding of added mass, Imlay²⁴ studied the basic principles and derived the complete expressions for the terms in the added mass matrix. The analysis revealed that the added mass terms are functions of the body size and shape, and density of the fluid as well as the vibrational mode shape and frequency. For a rigid body having six degrees of freedom, (ie. three translations and three rotations) the hydrodynamic added mass matrix is 6 x 6 containing 36 coefficients. The 36 coefficients are sometimes called the added mass derivatives, because they are related to the differentiation of the six components of the generalized hydrodynamic force with respect to the body's six acceleration components. Birkhoff²⁵ showed that for an ideal frictionless fluid, the general expressions for added mass contain only 21 independent coefficients so that the matrix becomes symmetric. Experience by some workers²⁶⁻²⁸ has shown that the numerical

values of added mass in a real fluid are usually in good agreement with those obtained for ideal fluid theory, depending of course on the degree to which the conditions of potential flow are met. For axisymmetrical or 2-D bodies, many of the 21 constants are identical to each other or equal to zero. Therefore, the hydrodynamic added mass for a rigid body may be represented by a 6 x 6 fully or partially populated symmetric matrix of coefficients.

The basic principles expressed by Imlay for a rigid body, can be generalized for a flexible structure that is partially or totally immersed in fluid. For each degree of freedom associated with the fluid-structure interface motions, there is corresponding fluid reaction force and moment components giving rise to generalized added mass coefficients for the body. These coefficients make up the general added mass matrix as expressed by equation (6). Thus, for a flexible structure with say 'n' degrees of freedom associated with the fluid-structure interface, the hydrodynamic added mass matrix is then n x n in size. This matrix is symmetric for an ideal fluid, fully populated for a 3-D structure and partially populated for a 2-D or axisymmetrical structure.

Although, the expressions derived by some authors show that the added mass coefficients may be proportional to the mass and moment of inertia of a specific characteristic volume of fluid, it should not be assumed that the added mass effects involve only that limited volume of fluid surrounding or moving with the body - the so-called "entrained fluid". Theoretically, all the particles of the fluid move, although the motion of the fluid is more pronounced in the neighbourhood of the body. As stated in Section 2.1, a sufficiently large region of fluid surrounding the body must be considered in developing the model for the mathematical analysis.

3. PREDICTIVE TECHNIQUES

3.1 Analytical Methods

Analytical expressions for the hydrodynamic added mass have been developed using classical aerodynamic or hydrodynamic potential flow theory or acoustic radiation impedance theory. Den Hartog²⁹ used Theodorsen's method³⁰ for determining added mass effects. This method is based on aerodynamic theory for oscillating 2-D airfoils. The added mass and moment of inertia are related to a cylindrical region of fluid surrounding the airfoil with diameter equal to the foil chordlength (see Figure 1). The 2-D potential flow theory has been applied directly to infinitely long plates and cylinders,³¹⁻³⁸ and

3-D axisymmetric bodies.^{2,24} Chordwise strip theory with aspect ratio or end correction factors has extended the applicability of the 2-D potential flow theory to plates of finite length^{27,28} as well as bodies of more cylindrical shape such as ship hulls.³⁹⁻⁴³ Boundary conditions have been introduced to handle bodies in channels or restricted water depth.⁴³⁻⁴⁶

The acoustic radiation theory^{22,23} has been applied to bodies of varying complexity. The added mass is related to the reactive component of the radiation impedance. For simple structures such as circular pistons, spheres and infinitely long circular cylinders, closed form solutions have been obtained in the form of series expansions^{22,23}. Approximate and asymptotic formulas have been extracted from the series solutions for small and large values of the acoustic frequency parameter, ka , where 'a' is a characteristic dimension of the body such as radius and k is the wave number ($2\pi/\lambda$) of the acoustic wave in the medium. The acoustic analysis is limited to 2-D and axisymmetrical bodies and field solutions. For bodies of more complex surface forms, numerical techniques have been employed to analyze the acoustic radiation pressures on the interface surface and in the surrounding fluid.⁴⁷

3.2 Empirical Methods

Various experimental apparatus and procedures using scale models or full size structures have been devised for conducting tests in air (or vacuum) and in water or other fluids. Generally, the natural frequencies of vibration for the rigid body or elastic structure are measured in air and in water. Assuming that the aerodynamic added mass is negligible, the hydrodynamic added mass can then be determined from the frequency ratio equation

$$\frac{f_w}{f_a} = \left[\frac{M}{M+m_A} \right]^{1/2} \quad (7)$$

where f_w and f_a are the natural frequencies of the body in water and in air, M is the mass of the body and m_A is the actual hydrodynamic added mass. This method assumes that all other parameters and conditions remain constant for the tests in both fluids. Thus, the frequency measurements must be conducted under carefully controlled and realistic conditions with careful attention given to the mounting arrangement, structural stiffness, body motions, method of exciting the body motions and resonances, and techniques for determining the modal patterns and frequencies.

Rather than use equation (7) directly, many researchers determine the value of an added mass coefficient or correction factor K_A which is defined either in terms of the theoretical hydrodynamic mass, M_A , or actual body mass M . Using the theoretical hydrodynamic mass coefficient $K_A = m_A/M_A$, equation (7) becomes

$$\frac{f_w}{f_a} = \left[\frac{M}{M + K_A M_A} \right]^{1/2} \quad (8)$$

This is a semi-empirical approach since a suitable analytical expression must be available for predicting M_A .

If the actual body mass is used, the added mass correction factor would be given by $K_A = m_A/M$. This would reduce equation (7) to a form where the frequency ratio is a function of the factor K_A . Originally, this approach was employed in marine propeller design with rather crude estimates of the hydrodynamic mass being 25 to 30% of the total propeller mass.⁴⁸ Designers tried to generalize this concept of taking $K_A = 0.25$ to 0.30 for all propellers, but this simple empirical value was limited as it did not cover all ranges of blade thickness, blade shape, pitch angle, blade material density, frequency and vibratory mode shape. Equations (7) and (8) can also be applied to rotational motion, where the moments of inertia would be substituted for the masses and the added inertia correction coefficient K_I would replace K_A .

3.3 Numerical Methods

The interaction between the vibrating structure and the surrounding fluid has been handled numerically using the finite element analysis formulation.^{5,20,21,43,49-66} The finite elements developed for structures have been extended to model the medium by developing various types of fluid finite elements.^{55-60,78} The basic theory of fluid-structure coupling has been given by Zienkiewicz.^{20,21}

A direct finite element formulation of the fluid-structure system governed by equations (1) and (2) has been undertaken, but this approach is mathematically complex even for relatively simple structures.^{5,61-64} Both the structural displacements and fluid pressure have to be treated as the unknowns, giving rise to excessive computer storage requirements. Furthermore, some of the matrices are unsymmetric resulting in computational difficulties in the solution techniques.

A more effective approach has been to consider the structure and fluid as two separate sub-systems.⁶⁵ The hydrodynamic terms in the structural equation are determined from a solution of the boundary value problem for the fluid domain. For fluid domains with simple geometry, the solution can be obtained explicitly in closed form. As is generally the case, however, the geometry is more complex and separate finite elements have been developed to model the fluid region and to obtain the structural interface values. This approach reduced the computational effort by reducing the number of unknowns handled in the computer at any one time.

Further simplification is possible by limiting the consideration to the vibrational characteristics of the structure and adopting the assumption of incompressibility and no surface waves for the fluid.⁵⁷⁻⁵⁹ The added mass matrix is then given by equation (6). The terms in the added mass matrix can be determined by modeling the fluid and interface with specially developed finite elements which are compatible with the structural finite element models. Since the mass matrix is symmetric, standard matrix methods are used to solve for the structural displacements.

Various special and general purpose finite element computer programs^{10-12,15,16,60,66} have been developed which include methods for modeling the fluid. It is apparent that the most time consuming task is establishing the finite element model for the fluid with a sufficient number of elements and appropriate boundary conditions. Automatic mesh modeling generators have been developed in a few special application programs.^{60,78} Thus it appears that the numerical approach in the form of the finite element method has, perhaps, the greatest versatility and potential to account for the fluid interaction with the structure.

4. DISCUSSION

Having identified the techniques available, the following is a discussion of the various methods and an evaluation of their conditions and appropriateness for predicting the added mass. The material available is discussed under various sections depending on their application to different geometric shapes such as 2-D and 3-D rigid bodies, plates, propellers, cylinders and ship hulls. A summary of the various methods for the different shaped structures is presented in Table IX with mention of References and appropriate Figures and Tables.

4.1 Two and Three Dimensional Rigid Bodies

The extensive tabulations of theoretical and experimental values of the hydrodynamic mass coefficient for various shaped rigid bodies undergoing translational motion are presented by Patton³¹ and Hagist³³ in Table I and by Fritz³² in Table II. The theoretical coefficients in Table I (marked "t" in the source column) have been derived from potential flow considerations or acoustic radiation theory and the experimental values (marked "e") were obtained from tests by approximating potential flow or radiation conditions. Therefore, these values of added mass are appropriate only for low frequency, rigid body translational motion. Higher frequency added mass loading data based on acoustic radiation theory presented by Beranek²² (see Figure 2) are available for plane circular pistons radiating on one or both sides. The added mass is related to the imaginary reactive component X_M by

$$M_A = X_M / 2\pi f_w$$

Figure 2 illustrates the significant variation of X_M with frequency parameter, ka . X_M can be obtained from the figure provided the following are known; 'a' the piston radius, ρ the fluid density and c the speed of sound in water.

As an example, consider an eight inch diameter piston driven so it is radiating on both sides at a frequency $f_w = 140$ Hz.

For water, with

$$c = 5000 \text{ ft/sec}$$

$$\rho = 62.4 \text{ lbm/ft}^3$$

$$\text{giving } ka = 2\pi f_w a / c = 0.06$$

$$\text{From Figure 1 } X_M / \pi a^2 \rho c = 0.05$$

$$\text{which gives } X_M = 5450 \text{ lbm/sec}$$

$$\text{and the added mass } M_A = X_M / 2\pi f_w = 6.2 \text{ lbm}$$

For comparison, if the piston is 0.5 inch thick and made from steel ($\rho_s = 488 \text{ lbm/ft}^3$), the mass of the piston would be 7.1 lbm. The added mass, therefore, represents a significant proportion of the total system mass. Note, that the same answer can be obtained from the expression in Table I

where the added mass for a flat circular disc is given by $\frac{8}{3} \rho a^3$.

No frequency correction is necessary ($K=1$) because ka or $\omega a/c = 0.06$.

4.2 Plates and Foils

As mentioned in Section 3.1, Theodorsen's aerodynamic 2-D airfoil theory³⁰ as presented by Den Hartog²⁹ is perhaps the simplest predictive method to use. This was used by Barton⁶⁷ for correcting cantilever plate vibrational data. Even though this concept seems rather simplistic, it has even been used in conjunction with highly developed finite element structural analysis computer programs like SESAM-69⁶⁶ for preliminary natural frequency analysis of simple foil shaped structures such as rudders, struts, fins and steerable nozzles (see Figure 1)⁶⁸. The savings in computational time and cost is substantial. However, for greater detailed analysis and more complex structures, SESAM-69 has an advanced fluid element numerical capability.

Lindholm, Kana, Chu and Abramson^{27,28} produced the most comprehensive set of test data available on the elastic vibrational characteristics of partially or totally immersed cantilever plates (see Figure 3). The first six natural frequencies in air and in water were determined for plates of various thickness and length. For the fully submerged condition, the frequency data is presented in Table III and as a non-dimensionalized frequency parameter in Figure 4 for modes 1 and 2. The added mass factors based on hydrodynamic strip theory for the six modes are given in Table IV. The results for partially immersed plates are summarized in Figure 5.

Lindholm et al found that the first bending natural frequency predictions (Figure 4(a)), using the strip theory added mass factors, required corrections based on aspect ratio and thickness effects as did the other flexural modes 3 and 6. The strip theory predictions, however, showed good agreement with experiment for the second mode frequency of 154 Hz, which is a torsional mode (Figure 4(b)). The other torsional modes 4 and 5 showed similar agreement without the need of corrections.

The results presented in Figure 5 illustrate the percent change in the plate resonant frequencies and the change in the location of the nodal lines with variation of the depth of immersion in water. The results in Figure 5(b) for horizontally submerged plates indicate that at depths greater than about 50% of the length, the resonant frequency has reached the deep water value. However, the results for surface piercing plates as shown in Figure 5(c) are much more sensitive to the mode of vibration, and the base of the plate must be fully submerged to reach the deep water value.

For detailed vibrational analysis of elastic plate structures, the numerical methods based on finite element theory presented by Zienkiewicz^{20,21} are the most concise predictive techniques. Chowdhury⁵⁷ extended the theory for vibrating plates by developing a 13 noded hexahedron fluid superelement as shown in Figure 6. This element provides for a natural coarsening of the finite element mesh for the fluid with increasing distance from the plate. This approach tends to minimize the number of nodal points and thus optimize the fluid model. Norwood's application⁵⁹ of the finite element method for the calculation of the hydrodynamic added mass of marine propeller blade is directly applicable to analysis of cantilever plates of any shape or size. This method is advantageous because it has an automatic element mesh generator for special plate forms such as propeller blades as well as a manual grid modeling capability for both the structure and the fluid. The application of the finite element program NASTRAN to the vibration of submerged plates by Marcus⁶¹ gives a good comparison of the finite element results with the experimental data of Lindholm et al^{27,28} as shown in Figures 7 and 8.

For preliminary design analysis of plate structures, the experimental data by Lindholm et al^{27,28} or the empirical formulas tabulated by Patton,³¹ Fritz³² and Hagist³³ may be sufficiently accurate besides being much simpler and cheaper to use than the finite element computer methods. However, detailed design analysis requires application of a finite element method such as that by Chowdhury, Norwood or Marcus. Selection of a solution method will depend on the particular problem and accuracy of the solution desired.

4.3 Marine Propellers

For marine propellers, extensive experimental and theoretical work has been conducted because of interest in blade vibrational characteristics, strength adequacy, propeller-hull interaction and radiated noise. Early design philosophies for longitudinal vibration of propeller shafting systems were examined by Kane and McGoldrick.⁴⁸ Initially, the propeller blade was considered to respond essentially as a flat plate with the blade thickness and section shape having negligible effects. Subsequently, it has been shown that the 3-D blade shape, tip effect, aspect ratio and vibrational mode are important parameters that cannot be accurately accounted for using flat plate results.

4.3.1 Complete propeller

Lewis et al⁶⁹ developed the following useful empirical formulas for hydrodynamic added mass and moment of inertia for conventional propellers undergoing axial and torsional motions:

$$M_A = \frac{0.21\rho D^3 (MWR)^2 n}{[1 + (P/D)^2][0.3 + MWR]} \quad (9)$$

$$M_A' = \frac{M_A}{1 + (P/2\pi)^2 \cdot M_A / I_P} \quad (10)$$

and $I_A = 0.8 M_A (P/2\pi)^2 = 0.02 M_A P^2$ (11)

where M_A is the predicted added mass of a propeller in axial motion with rotation restraint.

M_A' is the added mass of a propeller in axial motion with unrestrained shaft rotation.

I_A is the added polar mass moment of inertia for rotational motion.

I_P is the polar mass moment of inertia of the propeller structure (in vacuum)

D is the propeller diameter

P is the nominal propeller pitch

MWR is the mean width ratio (ratio of mean blade width to propeller diameter)

n is the number of blades

ρ is the fluid density

As mentioned by Lewis et al, M_A is the theoretical hydrodynamic added mass for a propeller. However, when a propeller is placed on a long flexible shaft M_A' should be used for frequency calculations because the pitch angle of the blades and the torsional flexibility of the shaft may couple in rotational motion to the axial motion. As an example, consider

a 3 bladed, 16 inch diameter, propeller with $P/D = 1.0$, $MWR = 0.42$ (blade area ratio equal to 0.65), $M_p = 13.5$ lbm and $I_p = 1.3$ lbm-ft². Using equations (9), (10) and (11), the axial added masses and torsional moment of inertia are predicted to be $M_A = 11.5$ lbm, $M'_A = 8.22$ lbm and $I_A = 0.41$ lbm-ft². Comparison with the propeller's mass and moment of inertia illustrates that the hydrodynamic added components are significant fractions of the propeller values.

Burrill and Robson⁷⁰ examined the effects of blade area ratio (B.A.R.) and pitch/diameter ratio (P/D) as shown in Figure 9 for a set of 16 inch diameter propellers with the number of blades ranging from 3 to 6. By using this extensive experimental data, Burrill found that Lewis' formulas (Equations (9) and (11)) were acceptable for B.A.R. less 0.6 and P/D less than unity, but failed to predict those for propellers having higher P/D and very wide blades.

Rather than using Lewis' formulas, Burrill developed correction factors K_I and K_A for the added inertia and mass, respectively, (Figure 10) based on Theoredorsen's fundamental airfoil theory^{29,30} (Sections 3.1 and 4.2). Burrill used the projected chord length as the dimension for the cylinder of fluid surrounding the blade and an end reduction factor which varied elliptically from the propeller axis to the blade tip to account for the 3-D effects. The correction factors K_I and K_A were found to be essentially independent of the pitch/diameter ratio, but as shown in Figure 10, they were functions of blade area ratio for the test propellers with 3 to 6 blades. Using the 3 bladed, 16 inch diameter propeller from the previous example, Theoredorsen's theory with elliptical spanwise distribution predicts that $M_A = 21.3$ lbm and $I_A = 0.96$ lbm-ft². Now with application of the correction factors from Figure 10 of $K_A = 0.65$ and $K_I = 0.60$, the added mass and inertia become $M_A = 13.8$ lbm and $I_A = 0.58$ lbm-ft². These corrected values of course agree with the experimental results that are shown in Figure 9 where $\theta_{2/3} = 26^\circ$ for the sample propeller.

What would appear to be more useful and easier to apply than Theoredorsen's theory and elliptical distribution are correction factors based on Lewis' formulas (Eqns (9) and (11)) and Burrill's experimental data. This was attempted for the 3, 4 and 5-bladed propellers as illustrated in Figure 11. In this case, using Lewis' formulas, the correction factors were found to be essentially independent of the blade area ratio and, to be instead, functions of the pitch/diameter ratio. As can be seen, the correction factors at high P/D are greater than unity indicating that Lewis' formulas underestimated the actual added mass and inertia. For the previous example of a 3-bladed 16 inch diameter propeller, Figure 11 indicates that $K_A = 1.17$ and $K_I = 1.38$. Using Eqns (9) and (11) and applying the correction factors, the predictions are $M_A = 13.5$ lbm and $I_A = 0.57$ lbm-ft², which agree well with Burrill's predictions.

As an extension, Norrie's work⁷¹ concentrated on torsional hydrodynamic inertia of a 3-bladed propeller using dimensional analysis and experimental measurements. Smoothed experimental inertia ratio results for various pitch settings (or P/D ratios) versus advance ratio J are shown in Figure 12. These data clearly illustrate the significant increase in the hydrodynamic inertia with pitch. A summary of the I_h/I_b data (ie. hydrodynamic inertia/propeller inertia) is given in Table V together with predicted values by Lewis, Burrill and others. An examination of the data indicates the typical increase in I_h with pitch. However, scatter, particularly at high P/D, is evident between the hydrodynamic inertia results predicted by the various authors' methods. As is apparent, Kane and Garibaldi's assumptions of I_h being 25 to 30% of I_b and independent of P/D are over-simplifications.

For a 3 bladed, 8 inch diameter, variable pitch propeller (B.A.R. = 0.675 and M.W.R. = 0.44) set at zero relative pitch of P/D = 0.96, Norrie's test results (Table V) give $I_h/I_b = 0.28$ compared to Lewis formulas of $I_h/I_b = 0.26$ (or 0.35 using correction $K_I = 1.36$ from Figure 11) and Burrill integration and correction factor prediction method of $I_h/I_b = 0.33$. Norrie attributed the scatter mainly to the limitations of the test and the simplifying assumptions such as two-dimensionality or other approximations that were introduced into the analytical or empirical expressions.

4.3.2 Propeller blade

Leggat and Sponagle⁷² were able to determine experimentally the effects of mass loading on the elastic resonant frequencies for a variety of propeller blades, using a striker and power spectrum analysis technique. Agreement of their frequency data with FEM numerically predicted frequencies⁶⁰ is better for modes 2 and 3 than for mode 1 (see Table VI). It appears that maintaining rigidity of the propeller blade mount and striker system, and the interpretation of the spectrum records for the natural frequencies of the blade are important factors in this type of measurement technique.

Altmann et al⁷³ have examined experimentally the performance of a few supercavitating propeller blades under typical cavitation conditions. The measurements indicated that the added mass coefficient for a blade with a complete cavity on the back face is less than half the value of that for a fully wetted blade. This significant reduction in the added mass is important in the frequency and dynamic response analyses of supercavitating blades because of the highly unsteady conditions under which they have to operate, particularly if the propeller is used in a semi-submerged operation.

Continuing interest in the detailed analysis of propeller vibration and strength has led to the development of suitable finite elements to model the blade and surrounding fluid. Under contract to DREA, Norwood⁶⁰ has developed a special purpose finite element program PVAST (Propeller Vibration And STrength) for vibrational and stress analysis of marine propeller blades of conventional and advanced geometries. As mentioned in Section 4.2, this program has the advantage of having an automatic element mesh generator as well as an interactive capability for describing the element mesh by using a digitizing graphics tablet. Calculation of the hydrodynamic added mass and inertia⁵⁹ is performed by modeling the surrounding fluid using the fluid and interface finite elements shown in Figure 13. The finite element mesh for a blade and fluid is given in Figure 14. The blade is indicated by the solid lines and the fluid elements by the dotted lines. The fluid surrounding the blade is limited to a region which would have maximum influence on the dynamic characteristics. The total depth of the fluid layers on either blade surface is typically one blade height and may be modeled with up to 5 layers. Two layers are shown in this illustration. For a controllable pitch propeller blade with leading or trailing edges that extend beyond the size of the palm base, the region below the base of the blade is modeled with fluid elements (Figure 14). For a conventional, fixed pitch blade, the two lower rows of fluid elements would be eliminated.

Norwood represented the mass of the surrounding fluid, given by equation (6), as a consistent mass matrix, which was then added to the nodal point structural mass of the blade. Predicted natural frequencies of two blades in air and in water are presented in Tables VI and VII. Comparison of the predicted frequencies with experimental data for the blades in air and in water indicates reasonable agreement. In Table VI, the discrepancy in the air natural frequencies for mode 1 is probably related to the experimental mounting arrangement for the blade, differences in modeling the blade root structure, and interpretation of the spectrum records as was suggested in the previous discussion of Leggat and Sponagle's work.

Blaker et al⁵⁸ has extended the application of the finite element method for submerged structures by developing suitable superelements for modeling the fluid region around a blade as shown in Figure 15. Chowdhury's superelement⁵⁷ (Figure 6) is also directly applicable to propeller blades. The fluid superelements provide a natural means of spreading or

coarsening the fluid element mesh. This improves the fluid model by being able to have a finer mesh near the blade and to model more of the region without having a larger number of nodal points and elements.

4.3.3 Summary of methods for propellers

DREA's experience is that the finite element numerical methods⁵⁷⁻⁶⁰ are vastly superior for predicting the added mass effects on the elastic vibrational characteristics of marine propeller blades. These methods, however, are more costly because of the amount of computer CPU time and massive working and core space required for an analysis. For preliminary propeller design, the experimental results by Burrill⁷⁰ and Norrie⁷¹, and empirical formulas by Lewis⁶⁹ with the correction factors given in Figure 11 may be sufficiently accurate especially for the complete propeller model. Selection of the appropriate method will depend, of course, on the particular problem and the accuracy of the solution required.

4.4 Cylinders and Ship Hulls

4.4.1 Empirical methods

In "Principles of Naval Architecture"³⁹, Lewis presented the basic principles of ship hull vibrations using empirical formulas to predict the hull elastic frequencies by taking into account the added mass for both vertical and transverse motions. Equations for vertical and transverse bending and torsional frequencies are given in the reference. The added mass per unit length for vertical heaving is given by

$$M_A = \rho \pi J C B^2 / 8 \quad (12)$$

where ρ = fluid density
 J = longitudinal reduction factor depending on mode
 C = section coefficient; $C = 1$ for a circular cylinder
 B = hull breadth at section waterline

The section coefficient C may be obtained either from Figure 16 by matching (ie. overlaying) the ship sections to one of the ship-like sections obtained by conformal transformation of a circle or by calculating the sectional area coefficient β and using Figure 17. For example, consider a section with a breadth-draft ratio $B/T = 2.0$ and the hull form sectional area coefficient $\beta = 0.785$, then from Figure 17 a value of $C = 1.0$ is obtained (ie. a circular cylinder). These sectional added mass data developed by Lewis are used extensively with strip theory to obtain the complete added mass factor for a ship's hull. It should be pointed out that this added mass

computation neglects the free surface wave effects, which introduce an oscillation frequency dependency. However, the 3-D effects of a ship's hull bending vibrations are accounted for by using the longitudinal reduction factor J derived from evaluation of an ellipsoid vibrating laterally in the two and three node modes, J_2 and J_3 respectively, or the vibration of a circular cylinder with up to 8 nodes (Figure 18). As can be seen, the reduction factor J and therefore the added mass decreases for the higher modes of vibration. This dependency on the mode of vibration is related to the relative longitudinal movement of the water.

As an application of Lewis' vibration analysis, consider for example a 400 foot, 4500 ton ship subdivided into 10 equal lengths as shown in Figure 19. The hull breadth $B = 50$ ft for all mid-sections except for the bow where $B = 30$ feet and the stern where $B = 46$ feet. The $B/2T$ is considered to be equal to 1.5 for all sections. By matching the three hull sections with Lewis' diagrams given in Figure 16, the section coefficients C were determined as recorded in Figure 19. Application of Equation (12) to each 40 foot section gives the total heave added mass

$$M_A = \frac{\rho \pi J}{8} 40 [0.90(30)^2 + 1.15(8)(50)^2 + 1.25(46)^2]$$

$$= 132,000 \rho \pi J = 25.9 \times 10^6 J \text{ lbm} = 11,600 J \text{ ton}$$

With $L/B = 8$ and using Lewis' results in Figure 18, the two and three noded bending mode reduction factors are $J = 0.82$ and $J = 0.76$. Therefore, the total heave added mass for the modes are

$$(2 \text{ noded mode}) M_A = 9490 \text{ ton}$$

$$(3 \text{ noded mode}) M_A = 8800 \text{ ton}$$

As evident, the predicted added mass is substantial being approximately twice the 4500 ton displacement of the ship. Therefore the vibration frequency in water as suggested by equation (8) (assuming $K_A = 1$) would be about 50% of the frequency in air. The same value of J for the 3 noded mode can be obtained from the cylindrical curve by Taylor (Fig. 18) where $\lambda/L = 0.72$ and $2\lambda/B = 11.52$. From the curve, J (3 nodes) = 0.76. Corresponding values of J for higher noded modes can be determined from the curve for a cylinder. For example, a 4 noded mode $\lambda/L = 0.5$ and $2\lambda/B = 8$ gives $J = 0.65$.

For transverse motion (sway), Lewis stated that the added mass is a less important factor than that for the vertical motion. As a result, for all ship sections close to circular shape and with the longitudinal axis at the water surface, an approximate expression for the added mass per unit length is derived from circular cylinder analysis as

$$(\text{sway}) M_A = 2\rho JT^2/\pi \quad (13)$$

where T is the draft. The value of the longitudinal reduction factor J for sway motion is not known accurately, but generally is assumed to be the values given in Figure 18 by substituting $B = 2T$.

As an example, consider the previous ship problem given in Figure 19. Using equation (13), the sway added mass is calculated to be

$$\begin{aligned} (\text{sway}) M_A &= \frac{2\rho J}{\pi} 40[10^2 + 8(16.6)^2 + (15.3)^2] \\ &= 4.03 \times 10^6 J \text{ lbm} = 1800 J \text{ ton} \end{aligned}$$

By using Figure 18 and substituting $L/B = L/2T = 12.0$, the longitudinal reduction factors are $J = 0.88$ and $J = 0.85$. Therefore, the total sway added mass for the modes are

$$\begin{aligned} (2 \text{ noded mode}) M_A &= 1580 \text{ ton} \\ (3 \text{ noded mode}) M_A &= 1530 \text{ ton} \end{aligned}$$

Note, that the sway added mass is substantially lower than the vertical heaving added mass or the tonnage displacement of the ship.

More recently, Madsen⁴³ has applied finite element numerical techniques for modeling the fluid (Figure 20) and beam theory for computing values of J for vertical heave vibration of ship-like sections. Results for two typical sections are presented in Figures 21(a) and 21(b) which indicate reasonable comparisons with other available data. Figure 22 shows the effect of limiting the water depth. As illustrated, there is a substantial increase in J due to restricted water depth.

Besides Madsen's results shown in Figure 22, the effect of water depth has been investigated by Yu and Ursell⁴⁴, and Kim⁴⁵ for 2-D circular and square cross-section cylinders. Kim converted measured hydrodynamic force data to added inertia coefficients for heave, sway and roll as shown by the sample results in Figures 23 and 24. As illustrated, restricting the water depth (h) increases the heaving added mass, but decreases the swaying and rolling added mass inertias except at low values of the frequency wave number $\nu = \omega^2/g$.

These data are useful for the calculation of ship motions in shallow harbours, rivers and canals.

As a specific case, the restricted water effect on sway added mass at essentially zero frequency (ie. quasi-steady) was predicted analytically by Flagg and Newman⁴⁶ for 2-D rectangular cylinders as shown in Figure 25. In this case, the sway added mass coefficient increases when restricting the water depth.

4.4.2 Potential flow methods

Hydrodynamic potential flow theory has been applied to the vibrational analysis of cylinders with ship-like sections by a number of researchers. Frank^{34,35} and Bedel³⁶ at DTNSRDC developed a method for calculating the added mass inertia and damping coefficients as functions of frequency for rigid cylinders oscillating in heave, sway and roll at or below the free surface. The oscillation frequency effects on the added mass and damping in the range of interest for ship motion is due to the free surface wave effects. The original work by Frank had two limitations, one involving frequencies at which the solution for semi-immersed bodies failed, and the other involving irregular shaped cylinders that could not be handled. Bedel improved the method to circumvent these initial limitations. This analytical method for calculating the sectional added mass together with strip theory is useful because it can be incorporated into a computer program and can handle a wide variety of ship-hull shapes.

As an extension of the potential flow, Landweber and Macagno^{37,38} used parametric and conformal mapping techniques to develop computer programs for predicting added mass of 2-D cylindrical forms vibrating horizontally and vertically at the free surface. Computer FORTRAN listings are given in their reports. Landweber^{40,41} then extended the analysis to flexible circular cylinders and bodies of revolution totally immersed in the fluid. As an example, the natural frequencies of the first 15 modes of vibration for a spheroid of axis ratio 9:1 were predicted using numerical matrix and strip theory methods to calculate the added mass. The matrix method can include both bending and shear energies in the structural analysis and, therefore, may be more accurate than the strip theory. However, evaluation and comparison of matrix and strip theory results with measured data were not found in the literature.

Complimentary work was done by Bishop et al⁴² in the U.K. using the strip theory method to represent the hydrodynamic added mass and fluid damping, and a modal beam analysis to model the structure. They were able to develop a theory which would predict the wave-induced vertical response of a flexible ship. The analysis was developed for a ship in a sinusoidal

sea. Nonetheless, Bishop states that for a ship in a random seaway, standard statistical methods can be applied provided an adequate statistical representation of the seaway can be described.

4.4.3 Finite element methods

Application of the finite element method to the structural analysis of ships has been extensive as indicated in the references.¹³⁻¹⁹ The impact of finite element techniques on practical design of ship structures is indicated in the paper by Roren.^{4,9} The basic principles for the computation of added mass have been presented by Zienkiewicz and Newton,²¹ Holand⁵⁰ and Newton et al⁵¹.

Application to the heaving motion of 2-D rigid cylinders submerged below or at the free surface is shown in Figure 26. The finite element numerical results are presented in Figure 27. Comparison with the theoretical prediction by Paulling and Porter⁷⁴, in Figure 27 as well as the measured C_H results by Kim (Figure 23(a)), verifies the accuracy of the finite element method.

For sway motion, Bai^{52,53} at DTNSRDC applied the finite element method to various 2-D cylinders in a canal as illustrated in Figure 28. He developed numerical solutions for the upper and lower bounds of the sway added mass at the zero and infinite frequency limits. Numerical results are tabulated in his report and the comparison with results by Fujino⁵⁴ is favourable. The zero frequency results of Bai for a rectangular cylinder with $B/2T = 1.0$ are shown in Figure 29 along with Flagg and Newman's curves from Figure 25. The resulting agreement is good.

Extending the analysis to 3-D structures, both Meijers⁵⁵ and Chowdhury⁵⁶ developed finite element models for the structure and fluid as illustrated in Figures 30 and 31. Comparison of the numerical and experimental results in Table VIII illustrates the accuracy of the finite element methods. These numerical techniques are easily adaptable to various 3-D shapes and therefore appear to be promising as methods for solving general vibrational problems.

As a means to handle general ship structure vibrational problems, special and general purpose finite element programs have been developed. Under contract to DREA, Norwood⁷⁸ has developed a special purpose finite element program HVA_{ST} (Hull Vibration And Strength) similar to the program PVA_{ST} for propeller blades (Sections 4.2 and 4.3.2). Program HVA_{ST} has automatic element mesh generators and digitizing graphics tablet capabilities for describing the

geometry and element meshes. For modelling and analysis, it has substructuring/superelement capabilities as well as extensive interactive pre-and post-processing programs for displaying the models and results of an analysis. Calculation of the hydrodynamic added mass⁵⁹ is performed using the same fluid and interface finite elements (Figure 13), and consistent mass matrix approach developed for the propeller program (see Section 4.3.2). SESAM-69⁶⁶ is also a special application program for marine structures that has suitable finite elements and superelement capabilities for modeling the fluid surrounding a ship hull. NASTRAN, a general purpose program developed in the U.S., mainly for the aerospace industry, has been developed in a limited way to handle the hydrodynamic fluid problems.

To predict the natural frequencies and mode shapes for propeller shaft bearing induced ship vibration, Liepins et al⁷⁵ modeled the ship structure as shown in Figure 32 and applied scalar mass elements available in NASTRAN to represent the fluid mass effects. This requires a prior knowledge of the hydrodynamic added mass either by some analytical or empirical means before attempting a solution.

Using NASTRAN, various methods have been specially applied to fluid-structure interaction by Everstine^{62, 63}, Zarda⁶⁴ and Coppolino⁶⁵ in which the fluid is treated as an acoustic medium ie., compressible, inviscid with small amplitude motion. Initially, application of the fluid pressure approach by Zienkiewicz and Newton²¹ required program modifications to NASTRAN and generated non-symmetric matrices. On the other hand, if fluid displacements are incorporated as the fundamental unknowns as proposed by Kalinowski, the standard version of NASTRAN can be used directly and the matrices generated are symmetric. However, this method requires three unknowns per fluid node rather than one (pressure) resulting in a penalty of large matrix size and bandwidth. The pressure analogue method proposed by Everstine et al⁶² uses standard elastic finite elements available in NASTRAN to model the fluid region in which the fluid pressure is represented by the x displacement variable and the material property matrix takes on a special isotropic form. This method requires that the pressure satisfies a particular boundary condition at the fluid-solid interface and an infinite fluid radiation damping condition be applied at a distance sufficiently far from the structure.

Everstine⁶³ also implemented another method, known as the decoupling doubly asymptotic approximation, to solve shock response problems for submerged structures. In this case, because interest is in the behaviour of the structure rather than the fluid, schemes are used to approximate the fluid effects without actually modeling the fluid. Analytical expressions in differential equation form describe the

relationship between the fluid pressure at the interface and the structural interface motion. This approach results in matrices of acceptable bandwidth but degrades numerical stability, requiring a smaller solution time step size, and therefore longer computer CPU time than would otherwise be used. It also requires program modifications which are not available in existing commercial versions of NASTRAN. Additional discussion of the fluid-structure interaction capabilities of NASTRAN has been presented by Kalinowski and Patel⁷⁶, who indicate that the present program's hydroelastic analyzer still uses essentially the fluid pressure approach of Zienkiewicz and Newton²¹, and the program's capability is restricted to modeling the fluid in 2-D and axisymmetric structural systems.

4.4.4 Summary of methods for cylinders and ship hulls

If interest is confined to a particular mode of vibration such as heave, sway or roll, the theoretical hydrodynamic potential flow methods developed by Frank^{34,35} and Bedel³⁶ at DTNSRDC can be applied for calculation of the added mass inertia and damping coefficient as a function of frequency.

For the cases of heave and sway motion and neglecting the free surface wave effects, the method by Lewis³⁹ is suggested together with Madsen's numerical techniques⁴³ for calculating the longitudinal reduction factor J. This method can also predict the increase in the value of J due to shallow water effects.

The computer FORTRAN programs developed by Landweber and Macagno^{37,38,40,41} could easily be implemented to predict the added mass effects for 2-D cylindrical and axisymmetric forms. Bishop's strip theory method⁴² using Lewis' added mass results may be a viable alternative for prediction of wave-induced vertical response since it accounts for the rotary inertia, and flexural and shear rigidities of a flexible ship structure.

The simple finite element methods like those developed by Meijers⁵⁵ and Chowdhury⁵⁶ are recommended for general design analysis because of the ease of modeling the structure and fluid, and the relatively short computer CPU time, low costs and small storage requirements. However, detailed vibrational analysis of the complete ship structure requires the use of large programs like SESAM-69⁶⁶ and NASTRAN^{62-65,75,76} which are time consuming and expensive to run.

CONCLUDING REMARKS

It is necessary in dynamic analysis of submerged structures to account for the effects of the hydrodynamic added mass inertia. The reduction of the vibrational frequency is substantial depending on the size and shape of the structure, the frequency and mode of vibration and the proximity of surrounding rigid and air interface boundaries.

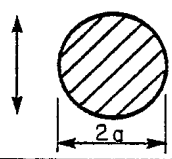
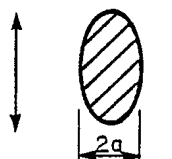
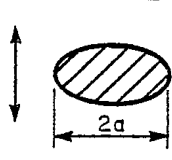
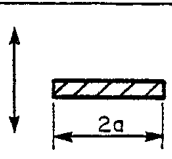
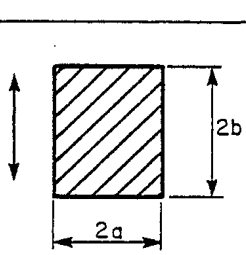
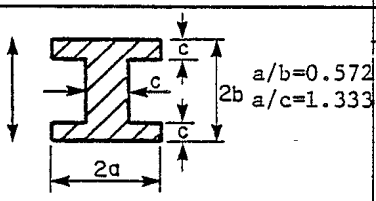
No one satisfactory universal method has been developed for calculation of the added mass effects. However, various predictive methods and measurement techniques can be used to handle many conditions and configurations of interest. For detailed analysis of the structural vibration and strength of naval architectural structures such as plates, foils, fins, struts, rudders, propellers, cylinders and ship hulls, the numerical finite element methods are vastly superior in predicting the added mass effects. General and special purpose finite element programs have been and are being developed which can model both the structure and surrounding fluid. Some programs have superelement capabilities to improve the modeling and advanced solution procedures. Automatic fluid element mesh generation is now available for marine propellers of conventional and advanced geometry using computer programs such as those developed by Norwood.^{59,60}

For conceptual and preliminary design analyses, simpler methods using analytical and empirical formulas may be sufficiently accurate besides being much faster and cheaper to use than finite element modeling of the fluid. These simpler methods, however, are limited to single modal motions such as bending, torsion, heave, sway or roll. Some are applicable only to 2-D or axisymmetric cases as well as being restricted to low frequencies. Application of the various methods, cited in this report, to various body shapes and vibrations are summarized in Table IX. Selection of a particular method will ultimately depend on the configuration and anticipated motion of the structure and the accuracy of the solution desired. The appropriate discussion in Section 4 should be consulted for selection of a suitable method with which to predict the hydrodynamic added mass inertia.

TABLE I

Hydrodynamic Mass of Various 2-D and 3-D Bodies

by Patton (Ref. 31)

TWO DIMENSIONAL BODIES																					
Section Through Body	Translational Direction	Hydrodynamic Mass per Unit Length	Source																		
	Vertical	$m_h = 1 \pi \rho a^2$	(4)t																		
	Vertical	$m_h = 1 \pi \rho a^2$	(4)t																		
	Vertical	$m_h = 1 \pi \rho a^2$	(4)t																		
	Vertical	$m_h = 1 \pi \rho a^2$	(4)t, (6)e																		
	Vertical	$m_h = K \pi \rho a^2$ <table border="0" style="margin-left: 20px;"> <tr> <td>a/b</td> <td>K</td> </tr> <tr> <td>∞</td> <td>1</td> </tr> <tr> <td>10</td> <td>1.14</td> </tr> <tr> <td>5</td> <td>1.21</td> </tr> <tr> <td>2</td> <td>1.36</td> </tr> <tr> <td>1</td> <td>1.51</td> </tr> <tr> <td>1/2</td> <td>1.70</td> </tr> <tr> <td>1/5</td> <td>1.98</td> </tr> <tr> <td>1/10</td> <td>2.23</td> </tr> </table>	a/b	K	∞	1	10	1.14	5	1.21	2	1.36	1	1.51	1/2	1.70	1/5	1.98	1/10	2.23	(4)t
a/b	K																				
∞	1																				
10	1.14																				
5	1.21																				
2	1.36																				
1	1.51																				
1/2	1.70																				
1/5	1.98																				
1/10	2.23																				
	Vertical	$m_h = 2.11 \pi \rho a^2$	(6)e																		

* m_h as used here is equivalent to M_A as used in text.

TABLE I (Cont.)

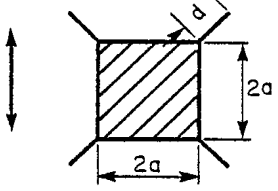
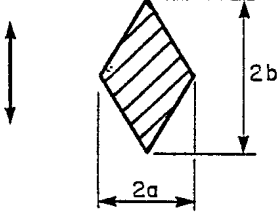
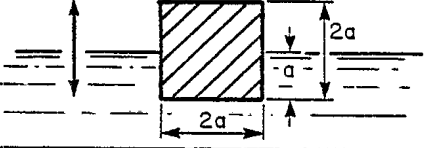
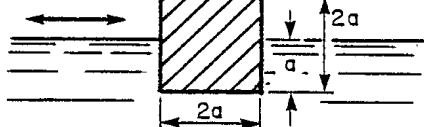
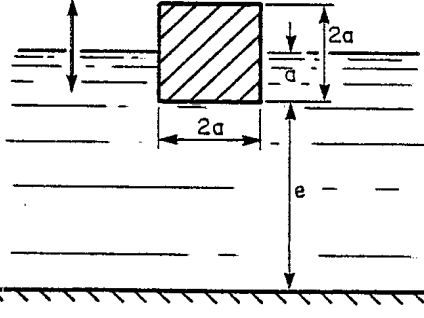
Section Through Body	Translational Direction	Hydrodynamic Mass per Unit Length	Source														
	Vertical	$m_h = K \pi \rho a^2$ <table border="0"> <tr> <td>d/a</td> <td>K</td> </tr> <tr> <td>.05</td> <td>1.61</td> </tr> <tr> <td>.10</td> <td>1.72</td> </tr> <tr> <td>.25</td> <td>2.19</td> </tr> </table>	d/a	K	.05	1.61	.10	1.72	.25	2.19	(4)t						
d/a	K																
.05	1.61																
.10	1.72																
.25	2.19																
	Vertical	$m_h = K \pi \rho a^2$ <table border="0"> <tr> <td>a/b</td> <td>K</td> </tr> <tr> <td>2</td> <td>.85</td> </tr> <tr> <td>1</td> <td>.76</td> </tr> <tr> <td>1/2</td> <td>.67</td> </tr> <tr> <td>1/5</td> <td>.61</td> </tr> </table>	a/b	K	2	.85	1	.76	1/2	.67	1/5	.61	(4)t				
a/b	K																
2	.85																
1	.76																
1/2	.67																
1/5	.61																
	Vertical (normal to free surface)	$m_h = .75 \pi \rho a^2$	(4)t														
	Horizontal (parallel to free surface)	$m_h = .25 \pi \rho a^2$	(4)t														
	Vertical (normal to free surface)	$m_h = K \pi \rho a^2$ <table border="0"> <tr> <td>e/b</td> <td>K</td> </tr> <tr> <td>∞</td> <td>.75</td> </tr> <tr> <td>2.6</td> <td>.83</td> </tr> <tr> <td>1.8</td> <td>.89</td> </tr> <tr> <td>1.0</td> <td>1.00</td> </tr> <tr> <td>.5</td> <td>1.35</td> </tr> <tr> <td>.25</td> <td>2.00</td> </tr> </table>	e/b	K	∞	.75	2.6	.83	1.8	.89	1.0	1.00	.5	1.35	.25	2.00	(4)t
e/b	K																
∞	.75																
2.6	.83																
1.8	.89																
1.0	1.00																
.5	1.35																
.25	2.00																

TABLE I (Cont.)

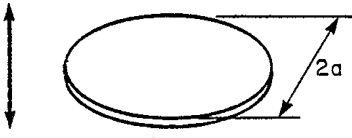
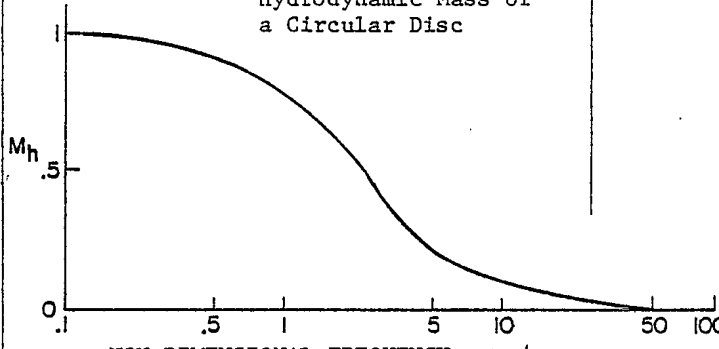
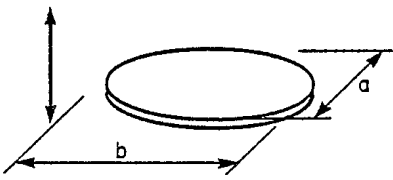
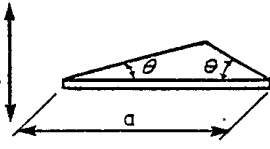
THREE DIMENSIONAL BODIES																																	
Body Shape	Translational Direction	Hydrodynamic Mass	Source																														
<p>1. <u>Flat Plates</u> Circular Disc</p>  <p>$c = \text{speed of sound in water}$</p>	Vertical	$m_h = K \frac{8}{3} \rho a^3$ <p>Effect of Frequency of Oscillation on Hydrodynamic Mass of a Circular Disc</p> 	<p>(1)t, (5)t</p> <p>(5)t</p>																														
<p>Elliptical Disc</p> 	Vertical	$m_h = Kba^2 \frac{\pi}{6} \rho$ <table border="1"> <thead> <tr> <th>b/a</th> <th>K</th> </tr> </thead> <tbody> <tr><td>∞</td><td>1.00</td></tr> <tr><td>14.3</td><td>.991</td></tr> <tr><td>12.75</td><td>.987</td></tr> <tr><td>10.43</td><td>.985</td></tr> <tr><td>9.57</td><td>.983</td></tr> <tr><td>8.19</td><td>.978</td></tr> <tr><td>7.00</td><td>.972</td></tr> <tr><td>6.00</td><td>.964</td></tr> <tr><td>5.00</td><td>.952</td></tr> <tr><td>4.00</td><td>.933</td></tr> <tr><td>3.00</td><td>.900</td></tr> <tr><td>2.00</td><td>.826</td></tr> <tr><td>1.50</td><td>.748</td></tr> <tr><td>1.00</td><td>.637</td></tr> </tbody> </table>	b/a	K	∞	1.00	14.3	.991	12.75	.987	10.43	.985	9.57	.983	8.19	.978	7.00	.972	6.00	.964	5.00	.952	4.00	.933	3.00	.900	2.00	.826	1.50	.748	1.00	.637	(7)t
b/a	K																																
∞	1.00																																
14.3	.991																																
12.75	.987																																
10.43	.985																																
9.57	.983																																
8.19	.978																																
7.00	.972																																
6.00	.964																																
5.00	.952																																
4.00	.933																																
3.00	.900																																
2.00	.826																																
1.50	.748																																
1.00	.637																																
<p>Triangular Plates</p> 	Vertical	$m_h = \frac{\rho a^3}{3 \pi} (\text{TAN}\theta)^{3/2}$	(6)e																														

TABLE I (Cont.)

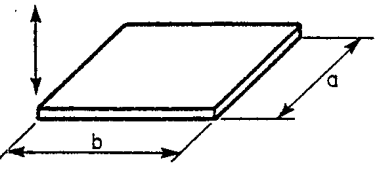

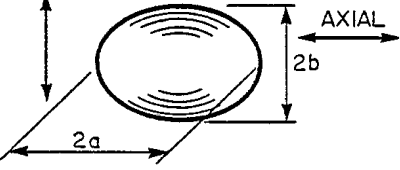
Body Shape	Translational Direction	Hydrodynamic Mass	Source																																										
<p>Rectangular Plates</p> 	Vertical	$m_h = K \pi \rho \frac{a^2}{4} b$ <table data-bbox="950 567 1161 808"> <thead> <tr> <th>b/a</th> <th>K</th> </tr> </thead> <tbody> <tr><td>1.0</td><td>.478</td></tr> <tr><td>1.5</td><td>.680</td></tr> <tr><td>2.0</td><td>.840</td></tr> <tr><td>2.5</td><td>.953</td></tr> <tr><td>3.0</td><td>1.00</td></tr> <tr><td>3.5</td><td>1.00</td></tr> <tr><td>4.0</td><td>1.00</td></tr> <tr><td>∞</td><td>1.00</td></tr> </tbody> </table>	b/a	K	1.0	.478	1.5	.680	2.0	.840	2.5	.953	3.0	1.00	3.5	1.00	4.0	1.00	∞	1.00	(6)e																								
b/a	K																																												
1.0	.478																																												
1.5	.680																																												
2.0	.840																																												
2.5	.953																																												
3.0	1.00																																												
3.5	1.00																																												
4.0	1.00																																												
∞	1.00																																												
<p>2. Bodies of Revolution Spheres</p> 	Vertical	$m_h = \frac{2}{3} \pi \rho a^3$	(1)t, (2)t																																										
<p>Ellipsoids</p> <p>VERTICAL</p> 	Vertical or Axial	$m_h = K \frac{4}{3} \pi \rho a b^2$ <table data-bbox="950 1281 1226 1732"> <thead> <tr> <th>a/b</th> <th>K for Axial Motion</th> <th>K for Vertical Motion</th> </tr> </thead> <tbody> <tr><td>1.00</td><td>.500</td><td>.500</td></tr> <tr><td>1.50</td><td>.305</td><td>.621</td></tr> <tr><td>2.00</td><td>.209</td><td>.702</td></tr> <tr><td>2.51</td><td>.156</td><td>.763</td></tr> <tr><td>2.99</td><td>.122</td><td>.803</td></tr> <tr><td>3.99</td><td>.082</td><td>.860</td></tr> <tr><td>4.99</td><td>.059</td><td>.895</td></tr> <tr><td>6.01</td><td>.045</td><td>.918</td></tr> <tr><td>6.97</td><td>.036</td><td>.933</td></tr> <tr><td>8.01</td><td>.029</td><td>.945</td></tr> <tr><td>9.02</td><td>.024</td><td>.954</td></tr> <tr><td>9.97</td><td>.021</td><td>.960</td></tr> <tr><td>10.00</td><td>.000</td><td>1.000</td></tr> </tbody> </table>	a/b	K for Axial Motion	K for Vertical Motion	1.00	.500	.500	1.50	.305	.621	2.00	.209	.702	2.51	.156	.763	2.99	.122	.803	3.99	.082	.860	4.99	.059	.895	6.01	.045	.918	6.97	.036	.933	8.01	.029	.945	9.02	.024	.954	9.97	.021	.960	10.00	.000	1.000	(1)t
a/b	K for Axial Motion	K for Vertical Motion																																											
1.00	.500	.500																																											
1.50	.305	.621																																											
2.00	.209	.702																																											
2.51	.156	.763																																											
2.99	.122	.803																																											
3.99	.082	.860																																											
4.99	.059	.895																																											
6.01	.045	.918																																											
6.97	.036	.933																																											
8.01	.029	.945																																											
9.02	.024	.954																																											
9.97	.021	.960																																											
10.00	.000	1.000																																											

TABLE I (Cont.)

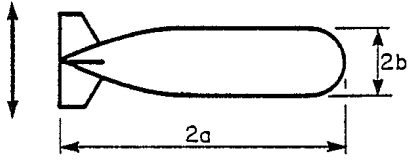
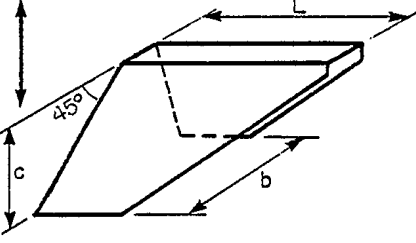
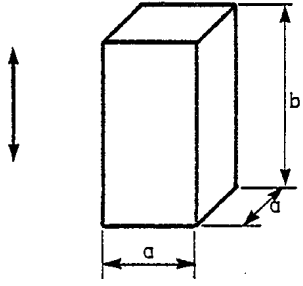
Body Shape	Translational Direction	Hydrodynamic Mass	Source																		
<p>3. <u>Bodies of Arbitrary Shape</u> <u>"Torpedo" Type Body</u></p> 	Vertical	$m_h = .818 \pi \rho b^2(2a)$ $a/b = 5.0$	(6)e																		
Area of Horizontal "Tail" = 10% of Area of Body Maximum Horizontal Section.																					
<p>V-Fin Type Body</p> 	Vertical	$m_h = .3975 \rho L^3$ $L/b = 1.0$ $L/c = 2.0$	(6)e																		
<p>Parallelepipeds</p> 	Vertical	$m_h = K \rho a^2 b$ <table border="0" data-bbox="950 1333 1144 1575"> <thead> <tr> <th>b/a</th> <th>K</th> </tr> </thead> <tbody> <tr><td>1</td><td>2.32</td></tr> <tr><td>2</td><td>.86</td></tr> <tr><td>3</td><td>.62</td></tr> <tr><td>4</td><td>.47</td></tr> <tr><td>5</td><td>.37</td></tr> <tr><td>6</td><td>.29</td></tr> <tr><td>7</td><td>.22</td></tr> <tr><td>10</td><td>.10</td></tr> </tbody> </table>	b/a	K	1	2.32	2	.86	3	.62	4	.47	5	.37	6	.29	7	.22	10	.10	(6)e
b/a	K																				
1	2.32																				
2	.86																				
3	.62																				
4	.47																				
5	.37																				
6	.29																				
7	.22																				
10	.10																				

TABLE I (Cont.)

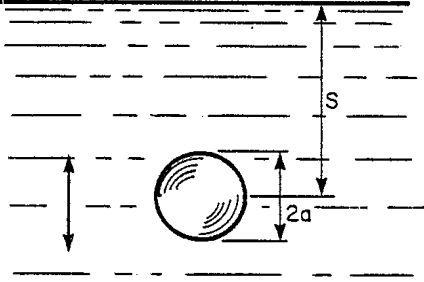
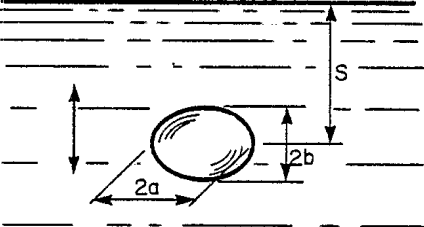
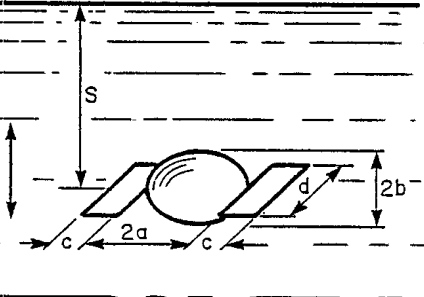
Body Shape	Translational Direction	Hydrodynamic Mass	Source																								
<p>Sphere Near a Free Surface</p> 	Vertical	$m_h = K \frac{2}{3} \pi \rho a^3$ <table border="1" data-bbox="954 499 1170 821"> <thead> <tr> <th>$s/2a$</th> <th>K</th> </tr> </thead> <tbody> <tr><td>0</td><td>.50</td></tr> <tr><td>.5</td><td>.88</td></tr> <tr><td>1.0</td><td>1.08</td></tr> <tr><td>1.5</td><td>1.16</td></tr> <tr><td>2.0</td><td>1.18</td></tr> <tr><td>2.5</td><td>1.18</td></tr> <tr><td>3.0</td><td>1.16</td></tr> <tr><td>3.5</td><td>1.12</td></tr> <tr><td>4.0</td><td>1.04</td></tr> <tr><td>4.5</td><td>1.00</td></tr> <tr><td>∞</td><td>1.00</td></tr> </tbody> </table>	$s/2a$	K	0	.50	.5	.88	1.0	1.08	1.5	1.16	2.0	1.18	2.5	1.18	3.0	1.16	3.5	1.12	4.0	1.04	4.5	1.00	∞	1.00	(6)e
$s/2a$	K																										
0	.50																										
.5	.88																										
1.0	1.08																										
1.5	1.16																										
2.0	1.18																										
2.5	1.18																										
3.0	1.16																										
3.5	1.12																										
4.0	1.04																										
4.5	1.00																										
∞	1.00																										
<p>Ellipsoid Near a Free Surface</p> 	Vertical	$m_h = K \frac{4}{3} \pi \rho ab^2$ <p>$a/b = 2.00$</p> <table border="1" data-bbox="954 1024 1170 1108"> <thead> <tr> <th>$s/2b$</th> <th>K</th> </tr> </thead> <tbody> <tr><td>1.00</td><td>.913</td></tr> <tr><td>2.00</td><td>.905</td></tr> </tbody> </table>	$s/2b$	K	1.00	.913	2.00	.905	(6)e																		
$s/2b$	K																										
1.00	.913																										
2.00	.905																										
<p>Ellipsoid with Attached Rectangular Flat Plates Near a Free Surface</p>  <p>$\frac{s}{2b} = 1.0$</p>	Vertical	$m_h = K \frac{4}{3} \pi \rho ab^2$ <p>$a/b = 2.00; c = b$</p> <p>$cd = N\pi ab$</p> <table border="1" data-bbox="954 1423 1170 1581"> <thead> <tr> <th>N</th> <th>K</th> </tr> </thead> <tbody> <tr><td>0</td><td>.9130</td></tr> <tr><td>.20</td><td>1.0354</td></tr> <tr><td>.30</td><td>1.3010</td></tr> <tr><td>.40</td><td>1.4610</td></tr> <tr><td>.50</td><td>1.5706</td></tr> </tbody> </table>	N	K	0	.9130	.20	1.0354	.30	1.3010	.40	1.4610	.50	1.5706	(6)e												
N	K																										
0	.9130																										
.20	1.0354																										
.30	1.3010																										
.40	1.4610																										
.50	1.5706																										

TABLE I (Cont.)

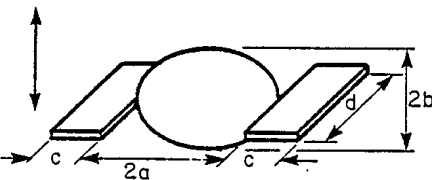
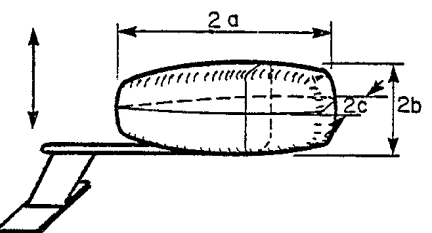
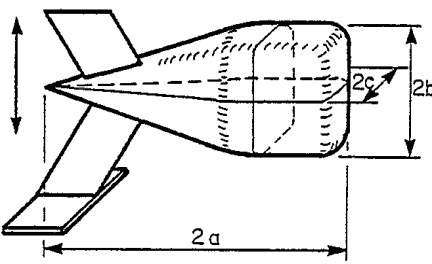
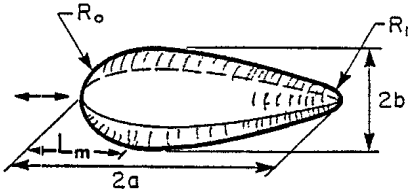
Body Shape	Translational Direction	Hydrodynamic Mass	Source												
<p>Ellipsoid with Attached Rectangular Flat Plates</p> 	Vertical	$m_h = K \cdot \frac{4}{3} \pi \rho ab^2$ $a/b = 2.00; c = b$ $cd = N \pi ab$ <table border="0" data-bbox="941 598 1161 766"> <tr> <td>N</td> <td>K</td> </tr> <tr> <td>0</td> <td>.7024</td> </tr> <tr> <td>.20</td> <td>.8150</td> </tr> <tr> <td>.30</td> <td>1.0240</td> </tr> <tr> <td>.40</td> <td>1.1500</td> </tr> <tr> <td>.50</td> <td>1.2370</td> </tr> </table>	N	K	0	.7024	.20	.8150	.30	1.0240	.40	1.1500	.50	1.2370	(6)e
N	K														
0	.7024														
.20	.8150														
.30	1.0240														
.40	1.1500														
.50	1.2370														
<p>Streamlined Body</p> 	Vertical	$m_h = 1.124 \rho \frac{4}{3} \pi ad^2$ $d = \frac{c + b}{2}$ $a/b = 2.38$ $a/c = 2.11$	(6)e												
<p>Area of Horizontal "Tail" = 25% of Area of Body Maximum Horizontal Section</p>															
<p>Streamlined Body</p> 	Vertical	$m_h = .672 \rho \frac{4}{3} \pi ad^2$ $d = \frac{c + b}{2}$ $a/b = 2.96$ $a/c = 3.46$	(6)e												
<p>Area of Horizontal "Tail" = 20% of Area of Body Maximum Horizontal Section</p>															

TABLE I (Cont.)

Body Shape	Translational Direction	Hydrodynamic Mass	Source
<p>Elongated Bodies of Revolution.</p>  <p>$m_h = K\rho V = K_e [1 + 17.0(C_p - 2/3)^2 + 2.49(M - 1/2)^2 + .283 [(r_o - 1/2)^2 + (r_1 - 1/2)^2]] \rho V$</p> <p>where; K - Hydrodynamic Mass coefficient for axial motion</p> <p>K_e - Hydrodynamic Mass coefficient for axial motion of an ellipsoid of the same ratio of a/b</p> <p>V - Volume of body</p> <p>C_p - Prismatic coefficient = $\frac{4V}{b^2(2a)}$</p> <p>L_m - Distance along body axis from nose to maximum cross-section</p> <p>M - Nondimensional abscissa = $L_m/2a$</p> <p>r_o, r_1 - Dimensionless radii of curvature at nose and tail</p> $r_o = \frac{R_o (2a)}{b^2} \quad r_1 = \frac{R_1 (2a)}{b^2}$	<p align="center">Axial</p>		
<p>For Vertical Motion:</p> <p>It has been shown that the hydrodynamic mass of an elongated body of revolution can be reasonably approximated by the product of the density of the fluid, the volume of the body and the K factor for an ellipsoid of the same a/b ratio.</p>			

List of References for Table I

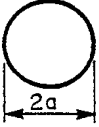
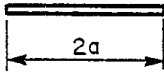
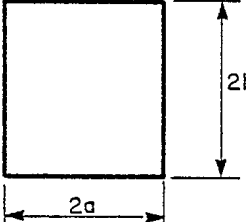
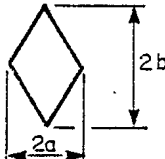
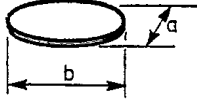
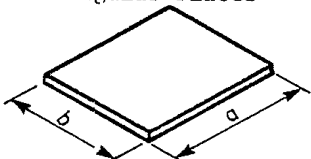
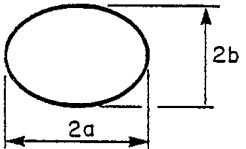
by Patton (Ref. 31) and Hagist (Ref. 33)

1. Lamb, H., Hydrodynamics, 6th. ed., Dover Publications, New York, 1945.
2. Birkhoff, G., Hydrodynamics, Princeton University Press, 1963.
3. Bramig, R., "Experimental Determination of the Hydrodynamic Increase in Mass in Oscillating Bodies," DTMB Translation 118, 1943.
4. Wendel, K., "Hydrodynamic Masses and Hydrodynamic Moments of Inertia," DTMB Translation 260, 1956.
5. Kinsler, L.E. and Frey, A.R., Fundamentals of Acoustics, 2nd. ed., John Wiley & Sons, Inc., N.Y., 1962.
6. Patton, K., "An Experimental Investigation of Hydrodynamic Mass and Mechanical Impedances," Thesis, University of Rhode Island, 1964.
7. Munk, M., "Fluid Mechanics, Part II," Aerodynamic Theory, Vol. I, edited by W. Durand, Dover Publications Inc., N.Y., 1963.
8. Landweber, L., "Motion of Immersed and Floating Bodies," Handbook of Fluid Dynamics, edited by V. Streeter, McGraw-Hill Book Company, Inc., N.Y., 1961.

Letters t and e listed under 'Source' indicate that the data was obtained from theory and experimentation.

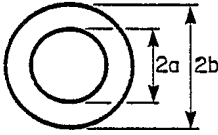
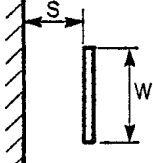
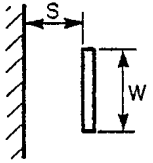
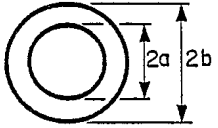
TABLE II

Hydrodynamic Mass by Fritz (Ref. 32)

Item	Direction of Motion	Hydrodynamic Mass	Ref.
1. Long Cylinder 	Vertical	$\pi\rho a^2$, per unit length	1
2. Thin Strip 	Vertical	$\pi\rho a^2$, per unit length	4
3. Rectangular Prism of Length L 	Vertical	a/b $K = \frac{M_H}{\pi\rho a^2 L}$	4
		∞ 1 10 1.14 5 1.21 2 1.36 1 1.51 1/2 1.70 1/5 1.98 1/10 2.23	
4. Diamond Section 	Vertical	a/b $K = \frac{M_H}{\pi\rho a^2}$ per unit length	4
		2 .85 1 .76 1/2 .67 1/5 .61	
5. Elliptical Disk 	Normal to Disk	b/a $K = \frac{M_H}{\frac{\pi}{6} \rho b a^2}$	4
		∞ 1.000 14.3 .991 6.00 .964 3.00 .900 1.50 .748 1.00 .637	
6. Rectangular Plates 	Normal to Plate	b/a $K = \frac{M_H}{\frac{\pi\rho a^2}{4} b}$	4
		1 .478 2 .840 3 1.000 ∞ 1.000	
7. Ellipsoid 	Vertical and Axial	$m_H = K \frac{4}{3} \pi \rho a b^2$	4
		a/b K K axial vertical 1.00 .500 .500 2.00 .209 .702 3.00 .121 .804 5.00 .059 .895 8.00 .029 .945 ∞ 0 1.000	

* M_H as used here is equivalent to M_A as used in text.

TABLE II (Cont.)

Item	Direction of Motion	Hydrodynamic Mass	Ref.
<p>8. Long Cylindrical Annulus of Length h</p> 	<p>Transverse to Axis</p>	$\frac{b^2 + a^2}{b - a} \rho \pi a^2 h \approx \frac{a}{c} \rho \pi a^2 h$ <p>$c = b - a$ $c \ll a$</p>	<p>1</p>
<p>9. Short Cylindrical Annulus - Axial Flow</p> <p>Annual Length h</p>	<p>Transverse to Axis</p>	$\frac{\pi \rho h^3 a}{12c}$ <p>$c = b - a; c \ll a$</p> <p>This annulus discharges axially into plena at each end.</p>	<p>8</p>
<p>10. Finite Length Thin Annulus Combination of Items 8 and 9</p>	<p>Transverse to Axis</p>	$M_H = \frac{a}{c} \frac{\rho \pi a^2 h}{1 + 12a^2/h^2}$ <p>This approximate formula checks within 0 to 12% higher than the three dimensional solution of Ref. 12 for $a/c = 9$.</p>	<p>8</p>
<p>11. Long Thin Annulus Surrounding Rotating Inner Cylinder</p>	<p>Transverse to Axis</p>	$\frac{\pi \rho a^3 h}{4c}$ (at critical speed) <p>$c =$ annulus thickness $a =$ annulus radius, $a \gg c$ $h =$ annulus length, $h \gg a$</p>	<p>11</p>
<p>12. Circular Disk near wall</p> 	<p>Lateral</p>	$\frac{\pi \rho a^4}{8s}$	<p>10</p>
<p>13. Long Thin Strip near wall</p> 	<p>Lateral</p>	$\frac{\rho w^3 L}{12s}$ <p>Length $L \gg w$</p>	<p>10</p>
<p>14. Concentric Spherical Annulus</p> 	<p>Vertical or Lateral</p>	$\frac{2}{3} \pi a^3 \rho \frac{b^3 + 2a^3}{b^3 - a^3}$	<p>1</p>

List of References for Table II


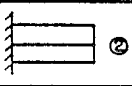
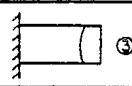
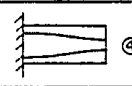
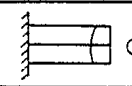
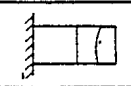
by Fritz (Ref. 32)

1. Stokes, G.G., "On Some Cases of Fluid Motion," Proceedings Cambridge Philosophical Soc., Vol. 8, May 1843, pp. 105-137.
2. Lamb, H., Hydrodynamics, 6th ed., Dover, 1945, ch. 6.
3. Birkhoff, G., Hydrodynamics, A Study in Logic, Fact, and Similitude, Princeton University Press, 1960, ch. 6.
4. Patton, K.T., "Tables of Hydrodynamic Mass Factors for Translational Motion," ASME Paper No. 65-WA/Unt-2, 1965.
5. Crandall, H., and McCalley, R.B., Numerical Methods of Analysis, Shock and Vibration Handbook, Vol. 2 (ed. C.M. Harris and C.E. Crede), McGraw-Hill, New York, N.Y.
6. Keane, J.A., "On the Elastic Vibration of A Circular Cantilever Tube in a Newtonian Fluid," PhD thesis, Carnegie Institute of Technology, Sept. 1963.
7. Moody, L.F., "Friction Factors for Pipe Flow," TRANS. ASME, Vol. 66, 1944, pp. 671-684.
8. Fritz, R.J., and Kiss, E., "The Vibration Response of a Cantilevered Cylinder Surrounded by An Annular Fluid," KAPL-M-6539, Feb. 1966.
9. McCalley, R.B., "Shock Analysis by Matrix Method, Notes for Short Course on Normal Modes," Shock and Vibration, Department of Engineering Mechanics, Pennsylvania State University, July 1966.
10. Private communication: items 12, 13 are due to J.H. Germer, General Electric Co.
11. Fritz, R.J., "The Effects of an Annular Fluid on the Vibrations of a Long Rotor, Part 1 - Theory; and Part 2 - Test," Journal of Basic Engineering, TRANS. ASME, Series D, Vol. 92, No. 4, Dec. 1970, pp. 923-937.
12. Kiss, E., "Analysis of the Fundamental Vibration Frequency of a Radial Vane Internal Steam Generator Structure," ANL-7685, Proceedings of Conference on Flow-Induced Vibrations in Reactor System Components, May 1970, Argonne National Laboratory, Argonne, Ill.

TABLE III

Natural Frequency Data for Fully Submerged Cantilever Plates in Air and Water
by Lindholm, Kana, Chu and Abramson (Ref. 27).

(For Notation see Figure 3)

PLATE			FREQUENCY - cps																				
NUMBER	a/b	h/d x 10 ²	MODE  ①						 ②			 ③			 ④			 ⑤			 ⑥		
			THEORY		EXPERIMENT		THEORY	EXPERIMENT		THEORY	EXPERIMENT		THEORY	EXPERIMENT		THEORY	EXPERIMENT		THEORY	EXPERIMENT			
			VACUUM	AIR	WATER	VACUUM	AIR	WATER	VACUUM	AIR	WATER	VACUUM	AIR	WATER	VACUUM	AIR	WATER	VACUUM	AIR	WATER	VACUUM	AIR	WATER
1	5	12.40	209	19.4	14.6	210	193	166	130	123	96				641	589	507	357	346	257			
2	2	6.11	65.7	60.7	40.3	283	267	209	409	377	257				922	858	645						
3	3	6.11	29.1	27.3	17.8	181	172	133	181	171	116				570	537	417	495	478	335			
4	5	6.11	10.4	10.0	6.3	105	99.6	77.3	65.2	62.3	40.1				321	306	226	178	175	114			
5	1	2.38	99.5	96.3	51.4	243	241	154	610	591	355	782	782	534	887	866	585						
6	2	2.38	24.7	24.2	12.1	106	108	67.5	154	151	80.0				347	348	222	419	422	243			
7	3	2.38	10.9	10.8	5.1	68.1	67.7	41.6	68.2	66.9	33.3				214	211	131	186	188	98.9			
8	5	2.38	3.93	3.84	1.78	39.5	39.1	24.2	24.5	24.2	11.5				121	121	75.2	67	68.1	33.5			
9	1/2	1.31	223	214	106	342	339	189	1397	1339	739	652	649	389	1580	1518	922						
10	1	1.31	55.6	52.9	23.3	136	129	68.7	341	326	158	437	423	234	496	476	267						
11	2	1.31	13.8	12.9	5.1	59.3	58.2	29.8	85.9	80.8	34.4				194	189	99.1	234	228	105			
12	3	1.31	6.11	6.2	2.3	38.0	40.3	20.6	38.1	38.7	15.4				120	126	65.7	104	109	46.5			
13	1/2	0.90	159	147	63.5	244	228	110	998	920	452	466	436	229	1129	1044	565						
14	1	0.90	39.7	37.9	14.6	97.1	95.3	44.2	243	236	102	312	299	155	354	344	174						
15	2	0.90	9.86	9.3	3.12	42.4	42.0	18.8	61.4	57.8	21.1				138	135	62.0	167	162	65.3			

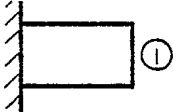
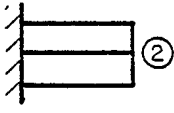
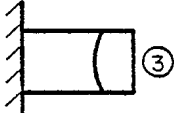
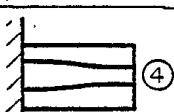
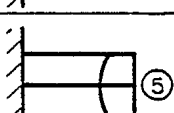
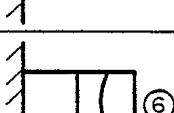
* PLATE THEORY; BARTON (4)
** BERNOULLI-EULER BEAM THEORY

TABLE IV

Predicted Added Mass Factors for Cantilever

Plates by Lindholm, Kana, Chu, and Abramson (Ref. 27).

(For Notation see Figure 3)

MODE	m	n	$\eta_{mn} = \sqrt{\frac{1}{1 + M_A/M}}$
 ①	1	0	$\sqrt{\frac{1}{1 + \frac{1}{4} \frac{\pi \rho b}{\rho_p h}}}$
 ②	0	1	$\sqrt{\frac{1}{1 + \frac{3}{32} \frac{\pi \rho b}{\rho_p h}}}$
 ③	2	0	$\sqrt{\frac{1}{1 + \frac{1}{4} \frac{\pi \rho b}{\rho_p h}}}$
 ④	0	2	$\sqrt{\frac{1}{1 + 0.0803 \frac{\pi \rho b}{\rho_p h}}}$
 ⑤	2	1	$\sqrt{\frac{1}{1 + \frac{3}{32} \frac{\pi \rho b}{\rho_p h}}}$
 ⑥	3	0	$\sqrt{\frac{1}{1 + \frac{1}{4} \frac{\pi \rho b}{\rho_p h}}}$

m = bending mode parameter

n = torsional mode parameter

η_{mn} = apparent mass factor = $\frac{\text{natural frequency in water}}{\text{natural frequency in air}}$

ρ = fluid density

ρ_p = propeller density

TABLE V

Comparison of Measured and Calculated Values of
 I_h/L_b For Rotational Motion of 3 Bladed Propeller
 By Norrie (Ref. 71). Measured Data Taken From Fig. 12

Pitch Setting deg.	P/D	Measured		Calculated (Various Formulas)					
		$R_e = 4.0$ to 6.0×10^5	Still Water	Kane	Garibaldi	Lewis	Burrill (integra- tion)	Burrill (formu- las)	Thomsen
-10	1.58	0.49	0.50	0.25-0.30	0.25	0.39	0.59	0.73	0.65
- 5	1.20	0.39	0.41	0.25-0.30	0.25	0.32	0.45	0.51	0.50
0	0.96	0.28	0.30	0.25-0.30	0.25	0.26	0.33	0.37	0.37
+ 5	0.74	0.21	0.22	0.25-0.30	0.25	0.19	0.23	0.24	0.26
+10	0.53	0.16	0.15	0.25-0.30	0.25	0.12	0.14	0.13	0.16

TABLE VI

DREA Comparison of Measured (Ref. 72) and Numerically Predicted (Ref. 60)
Natural Frequencies (Hz) for DTNSRDC 4580 Blade
On Conical Palm

MODE	IN AIR		IN WATER	
	FEM	EXP	FEM	EXP
1	498	659	328	328
2	1140	1155	788	635
3	1650	1693	1120	983
4	2190	1908	1550	

Blade Shape Shown in Fig. 14

TABLE VII

Comparison of Numerically Predicted and
Measured Natural Frequencies (Hz)

For DNV Blade (Ref.77)

MODE	DREA	
	FEM	
	AIR	WATER
1	135.1	47.9
2	389.5	177.1
3	426.4	195.3

DET NORSKE VERITAS			
FEM		EXP	
AIR	WATER	AIR	WATER
136.2	49.2	135.8	51.5
356.0	131.6		
436.2	183.4		

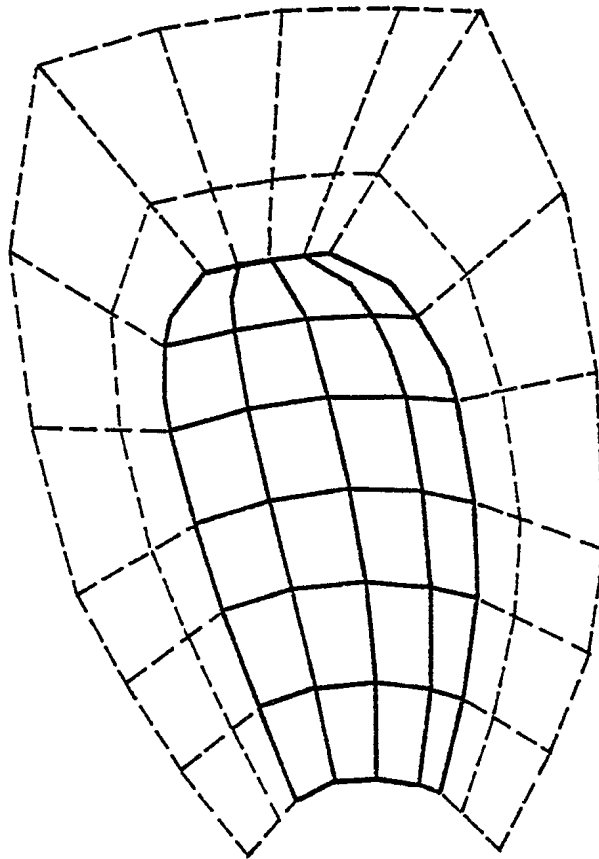


TABLE VIII

Measured and Numerically Predicted Natural Frequencies (Hz) in Water

For (a) Ship-Hull Shaped Structure by Meijers (Ref. 55)

(Fig. 30) and (b) Free-Free Box by Chowdhury (Ref. 56) (Fig. 31)

(a)

MODE NO.	FEM	MEASURED
1	1.51	1.4 (not accurate)
2	2.53	2.46
3	3.32	3.34
4	4.67	4.15

FEM	EXPERIMENTAL
101.0	112.4
206.9	208.6
317.8	325.7
325.2	335.9
404.8	439.0
472.7	466.8
522.1	-
524.0	-
571.0	586.8
627.8	699.4
672.5	-
716.6	828.4
723.8	-
910.3	886.5
954.7	-
997.4	1069.6
1008.5	-
1081.5	1196.5
1129.2	-
1129.3	-

TABLE IX

Summary of the Methods for Determining
The Hydrodynamic Added Mass Inertia of Various Shaped Bodies
Undergoing Various Types of Motions

BODY	MOTION	REPORT TABLES & FIGURES	REFERENCE NO.
2-D and 3-D RIGID BODIES	Low frequency translational motion	Tables I and II	Tabular expressions Refs. 31 to 33.
CIRCULAR PISTONS	Lateral motion frequency curves	Table I and Figure 1	22 and 31
<u>PLATES and FOILS</u> 2-D and 3-D forms	Low frequency, lateral motion	Tables I and II	29, 30, 31 and 32
Cantilevered (fully submerged)	First 6 bending and torsional modes	Tables III and IV Figures 3 and 4	27 and 28
Shallow or Partially submerged	First 6 bending and torsional modes	Figures 5, 7 and 8	27, 28 and 61
General	Elastic vibrations and dynamic response	Figures 6, 7 and 8	57, 59 and 61
<u>PROPELLERS</u> Conventional	Axial and rotational rigid body motion of propeller	Figures 9 and 10 or Equations 9 and 11 and Figure 11	69 and 70
Conventional	Rotational motion	Figure 12 and Table V	71
Supercavitating (blade with cavity on back)	Lateral motion	-	73
Blades of any geometry	Rigid motion or elastic vibrations of blades	Figures 6, 13 to 15 Tables VI and VII	57 to 60 and 77
<u>CYLINDERS AND SHIP HULLS</u> General 2-D hull forms	Vertical (heaving) bending vibrations	Figures 16, 17, 18, 23 and 27	39, 43 and 51
General 2-D hull forms	Transverse (sway) bending vibrations	Figures 16 to 18	39
2-D cylinders	Heave, sway, roll frequency dependency	Figures 23 and 24	34 to 36 and 44 to 46
2-D cylinders	Heave, sway, roll water depth effects	Figures 22 to 25	43 to 46

TABLE IX (Cont.)

BODY	MOTION	REPORT TABLES & FIGURES	REFERENCE NO.
2-D cylindrical forms	Heave, sway	Computer programs in References	37 and 38
Bodies of revolution	Flexural vibrations	Computer programs in References	40 and 41
Ship hull	Flexural, vertical wave response	-	42
2-D cylinders floating or submerged	Sway motion	Figure 29	50 to 53
General 3-D structures	Elastic vibrations	Figures 30 to 32 Table VIII	55, 56, 62 to 66, 75 and 76

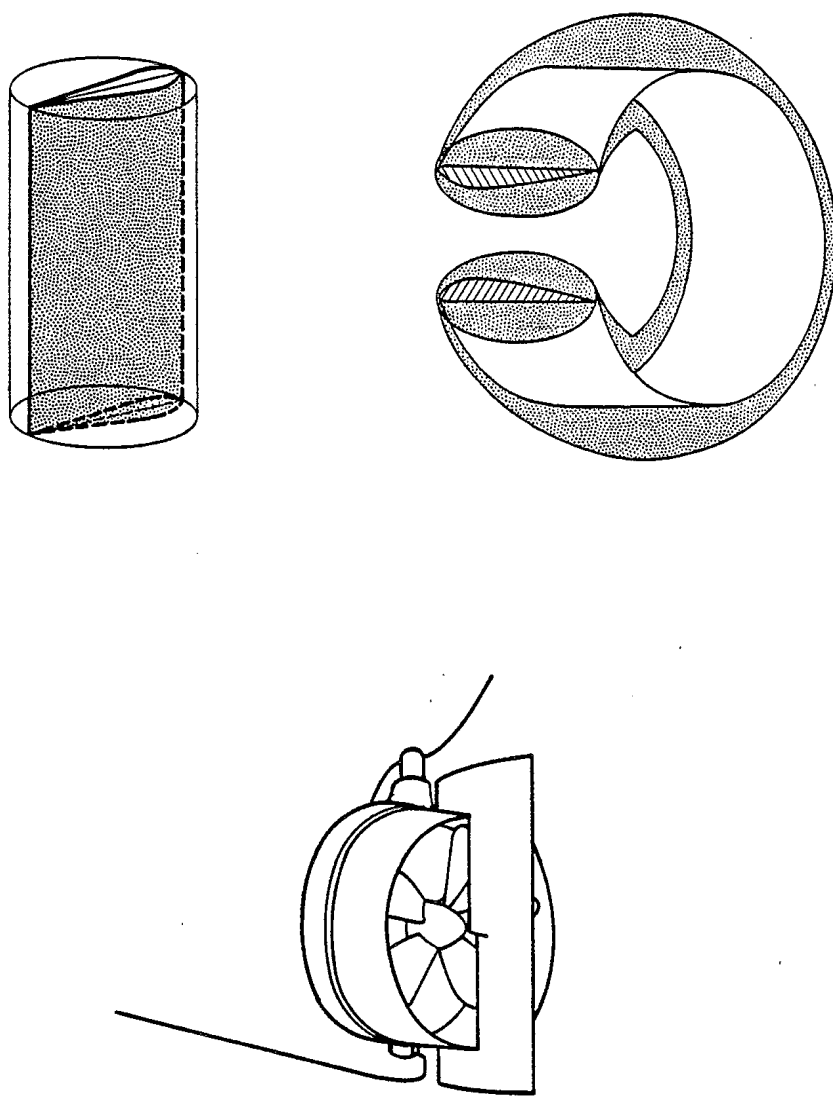


FIG.1 APPLICATION OF THEODORSEN'S 2-D AIRFOIL MODEL OF THE FLUID AROUND A NOZZLE AND RUDDER (REF.68).

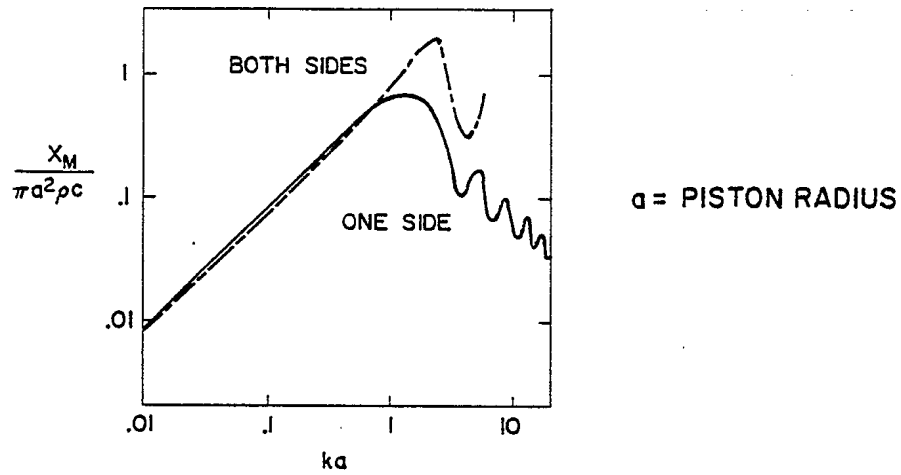


FIG.2 IMAGINARY COMPONENT X_M OF THE RADIATION IMPEDANCE OF A CIRCULAR PISTON RADIATING FROM ONE SIDE OR BOTH SIDES BY BERANEK (REF.22).

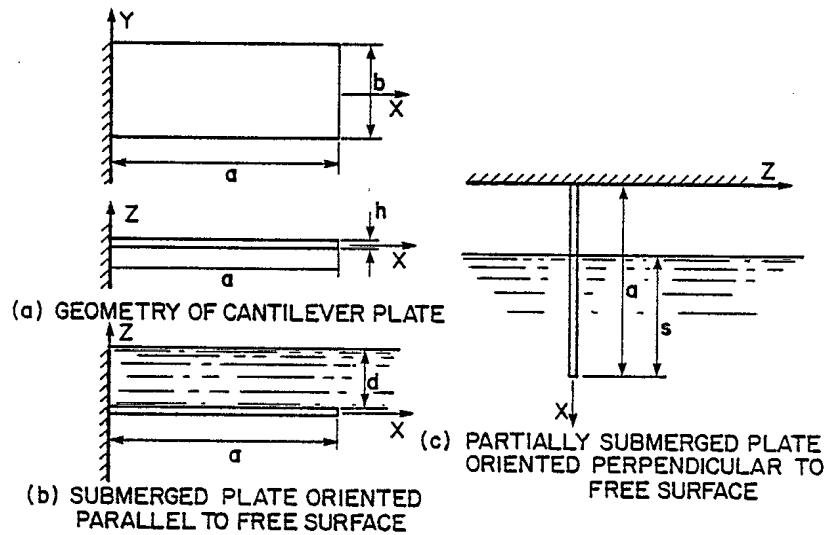
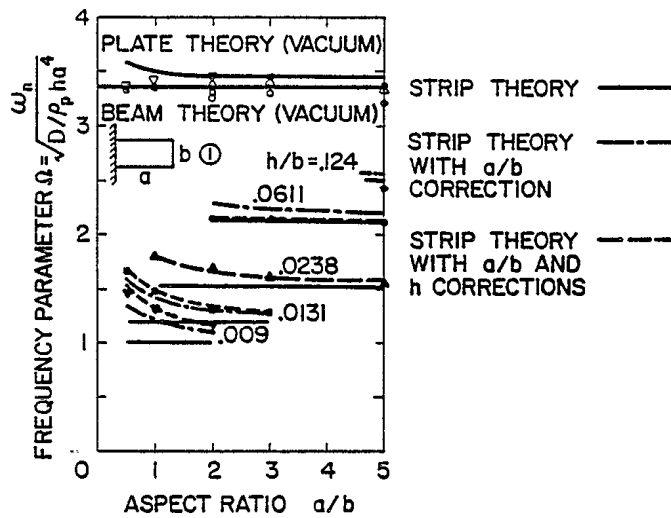
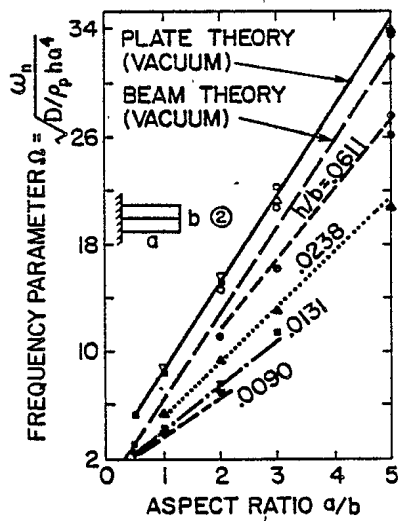


FIG.3 GEOMETRY OF CANTILEVER PLATE AND ORIENTATIONS WITH RESPECT TO LIQUID FREE SURFACE BY LINDHOLM, KANA, CHU AND ABRAMSON (REF.27 AND 28). (NOTATION APPLICABLE TO FIGURES 4,5,7 AND 8 AND TABLES III AND IV).

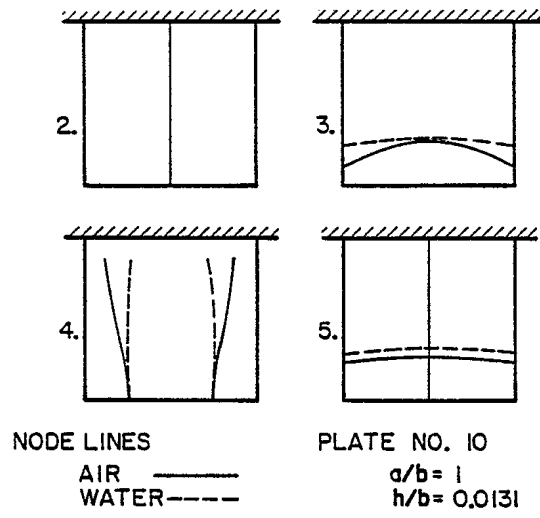


(a) BENDING (MODE 1)

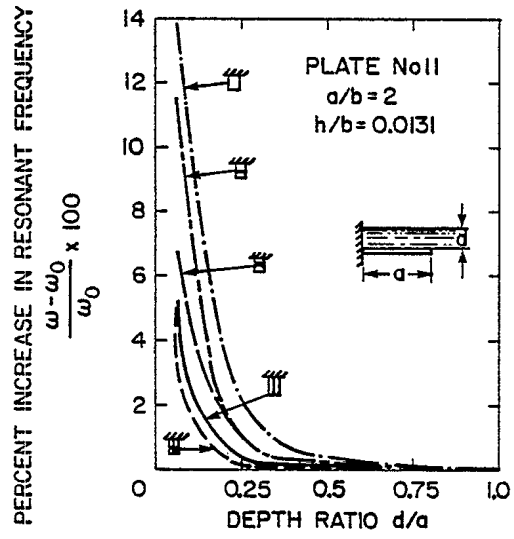


(b) TORSIONAL (MODE 2)

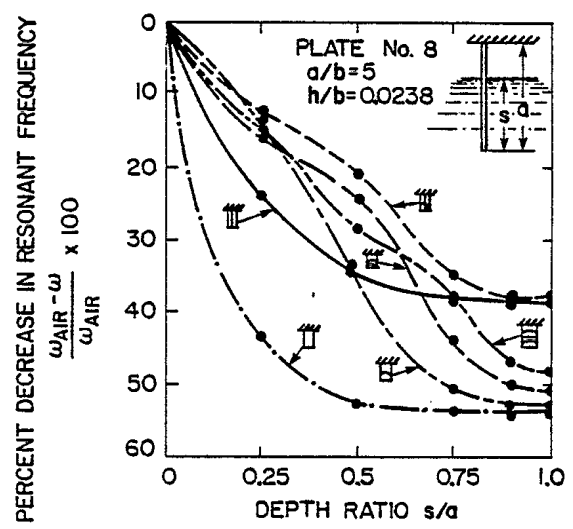
FIG. 4 NATURAL FREQUENCY RESULTS OF CANTILEVER PLATES BY LINDHOLM, KANA, CHU AND ABRAMSON (REF. 28).



(a)

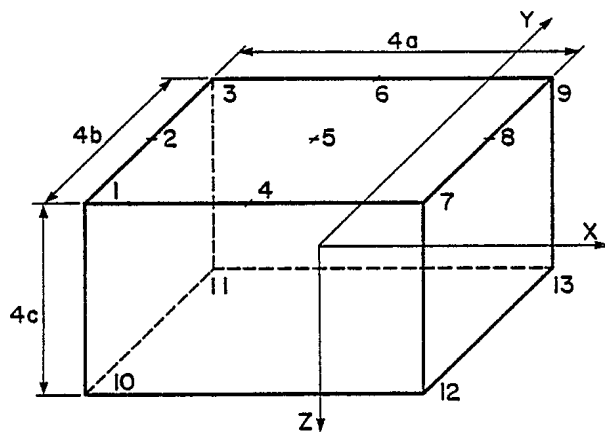


(b)

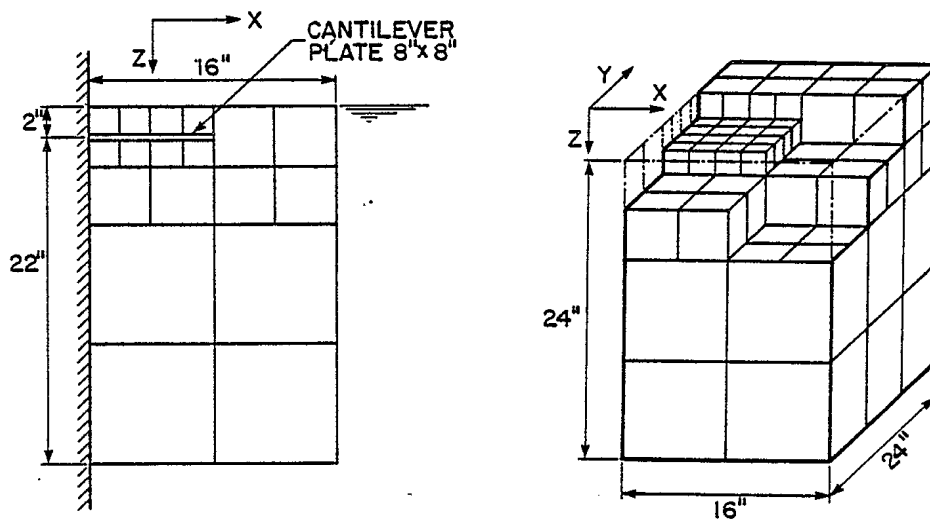


(c)

FIG. 5 (a) CHANGES IN (a) NODAL LINE LOCATIONS, AND (b) AND (c) RESONANT FREQUENCIES FOR SUBMERGENCE OF CANTILEVER PLATES BY LINDHOLM, KANA, CHU AND ABRAMSON (REF. 28).



(a)



(b)

FIG.6 (a) 13-NODED SUPERELEMENT AND (b) FINITE ELEMENT MODELING OF CANTILEVER PLATE AND FLUID BY CHOWDHURY (Ref.57).

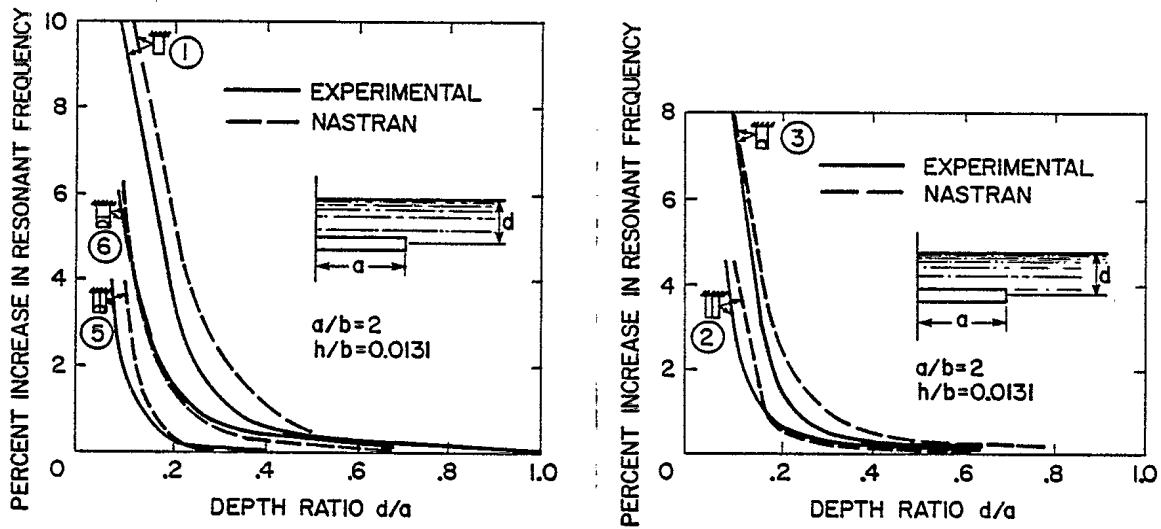


FIG. 7 PERCENTAGE INCREASE IN RESONANT FREQUENCIES WITH PROXIMITY TO LIQUID FREE SURFACE FOR CANTILEVER PLATE BY MARCUS (REF.61).

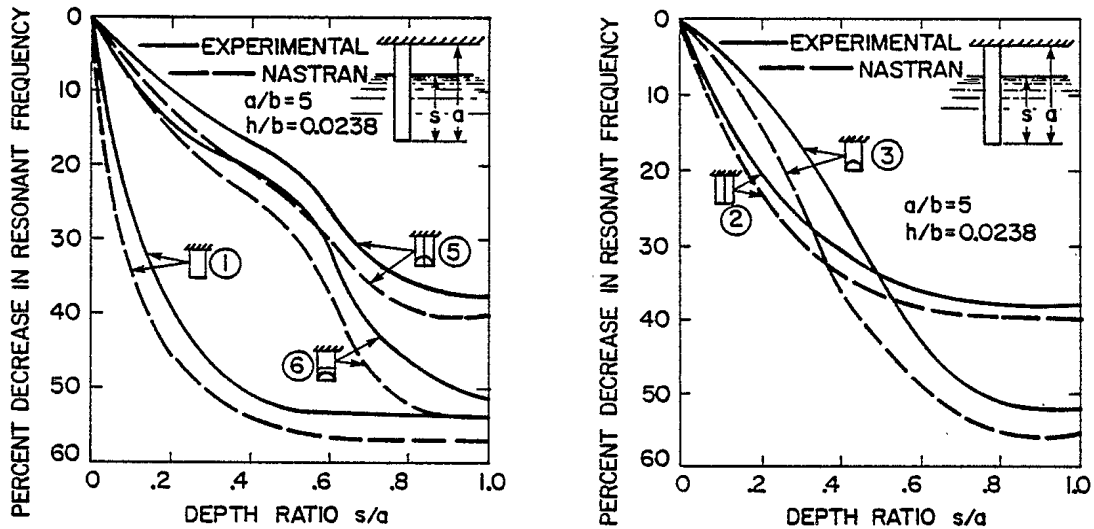
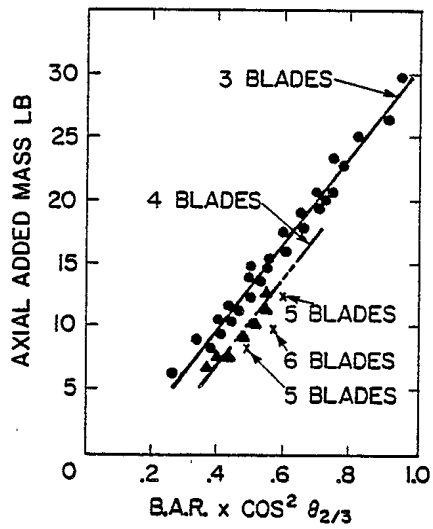
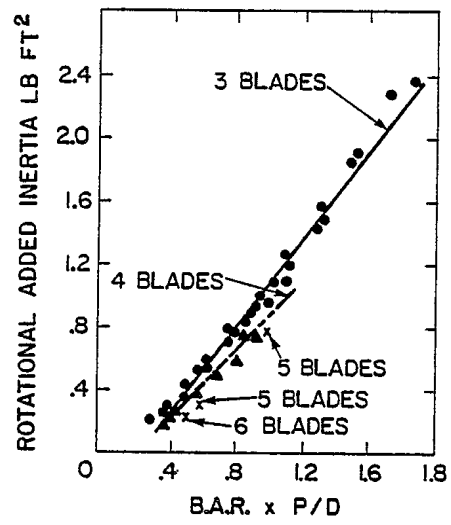


FIG. 8 PERCENTAGE DECREASE IN RESONANT FREQUENCIES WITH DEPTH OF IMMERSION FOR SURFACE-PIERCING PLATE BY MARCUS (REF.61).



(a)



(b)

FIG.9 MEASURED (a) AXIAL ADDED MASS AND (b) ROTATIONAL ADDED MOMENT OF INERTIA FOR 3,4,5 and 6 BLADED PROPELLERS BY BURRILL AND ROBSON (REF.70).

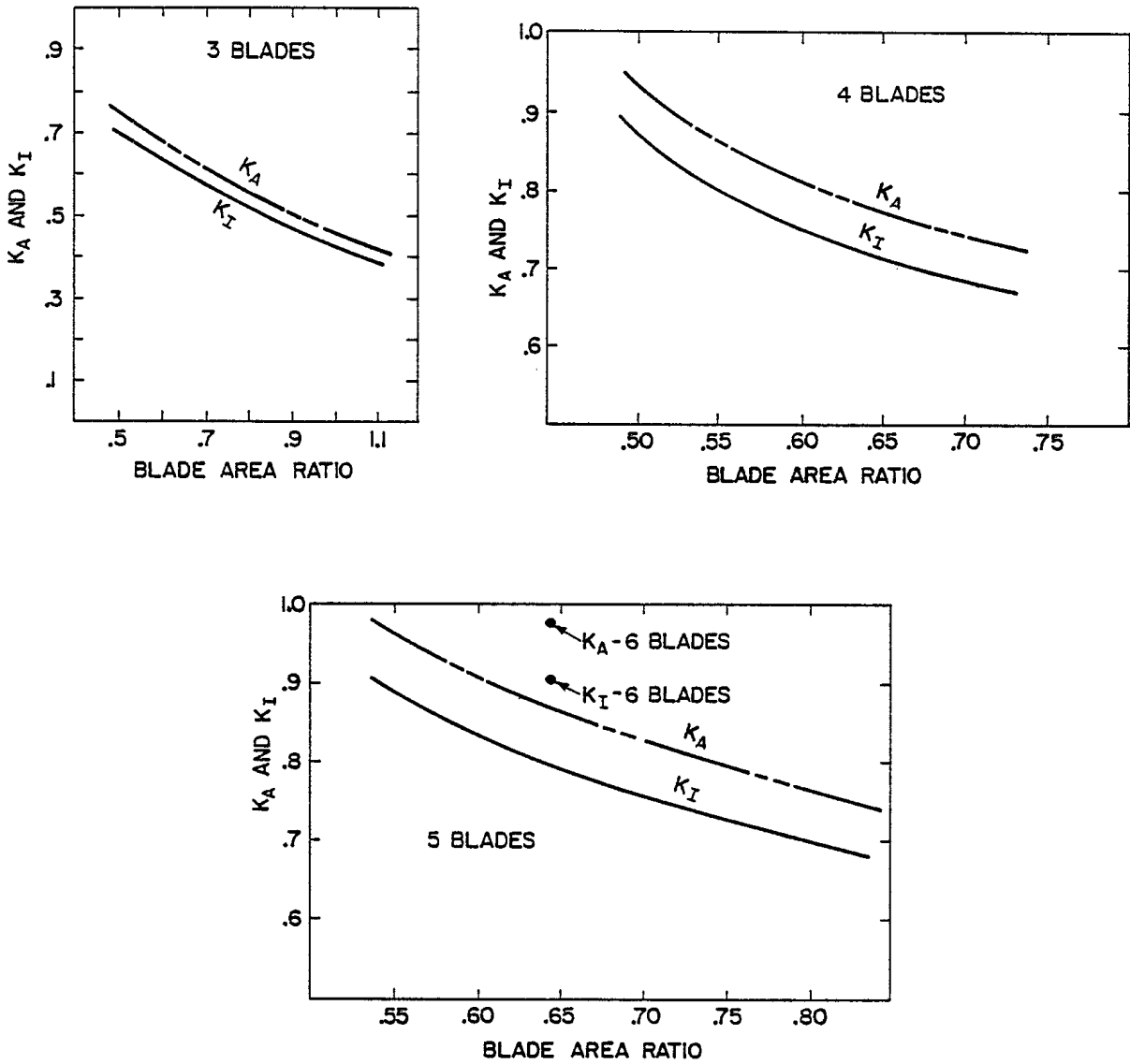


FIG.10 ADDED MASS AND INERTIA CORRECTION FACTORS K_A AND K_I AS FUNCTIONS OF BLADE AREA RATIO FOR 3,4,5 AND 6 BLADED PROPELLERS BY BURRILL AND ROBSON (REF.70)

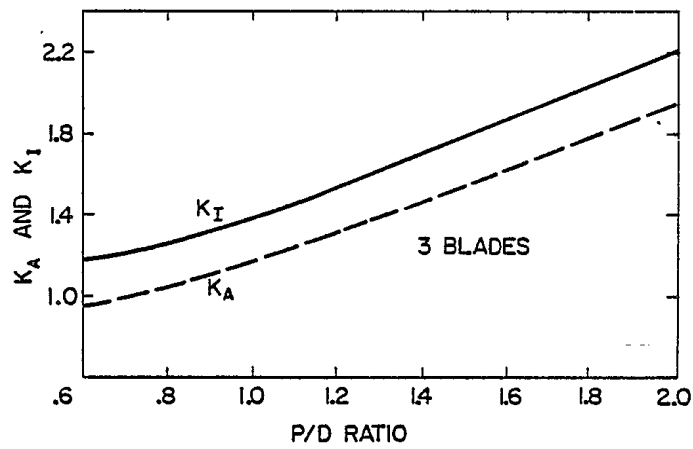
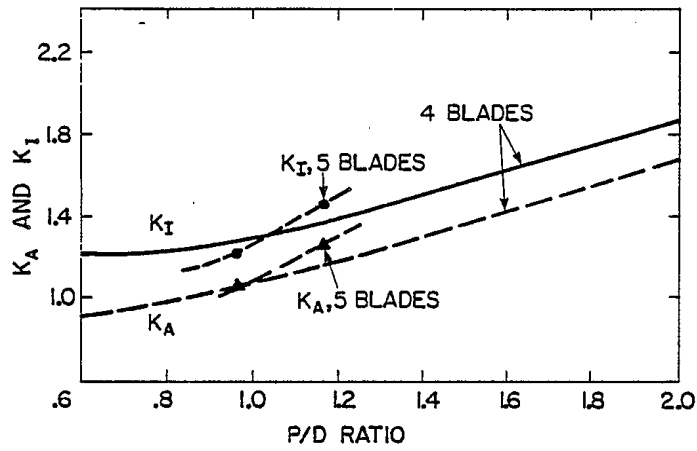


FIG.11 ADDED MASS AND INERTIA CORRECTION FACTORS K_A AND K_I BASED ON LEWIS'S FORMULAS EQNS. (9) AND (11) (REF.69), AND BURRILL AND ROBSON'S EXPERIMENTAL DATA (REF.70).

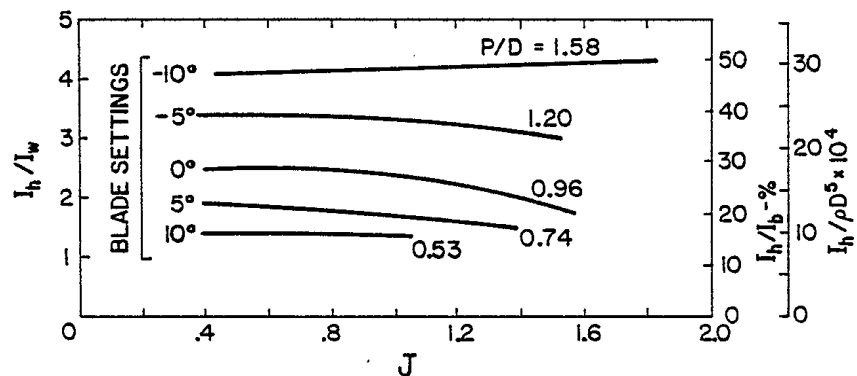


FIG.12 NONDIMENSIONALIZED HYDRODYNAMIC ADDED MOMENT OF INERTIA I_h WITH RESPECT TO FLUID DENSITY AND PROPELLER DIAMETER, AND RATIOS OF I_h TO THE EQUIVALENT BLADE DISPLAYED WATER MOMENT OF INERTIA I_w , AND THE BLADE METAL MOMENT OF INERTIA I_b FOR ROTATIONAL MOTION OF A 3-BLADED PROPELLER AT VARIOUS SETTINGS BY NORRIE (REF.71). DATA OF I_h/I_b IS SUMMARIZED IN TABLE V.

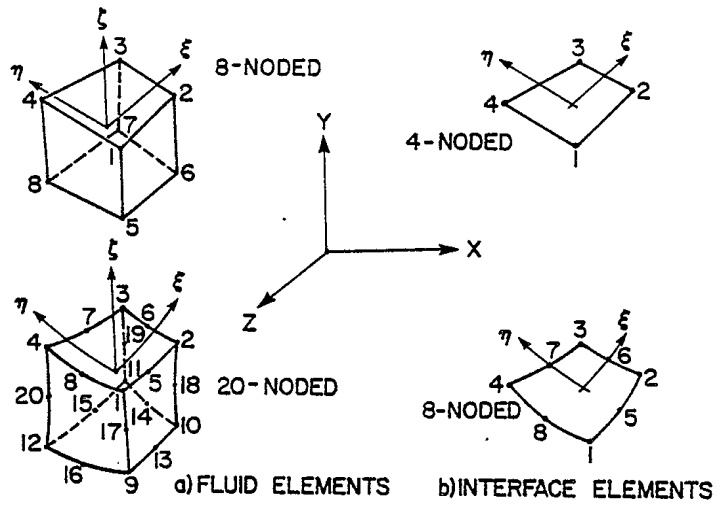


FIG.13 FLUID AND INTERFACE ELEMENTS FOR MODELING THE WATER BY NORWOOD (REF.59).

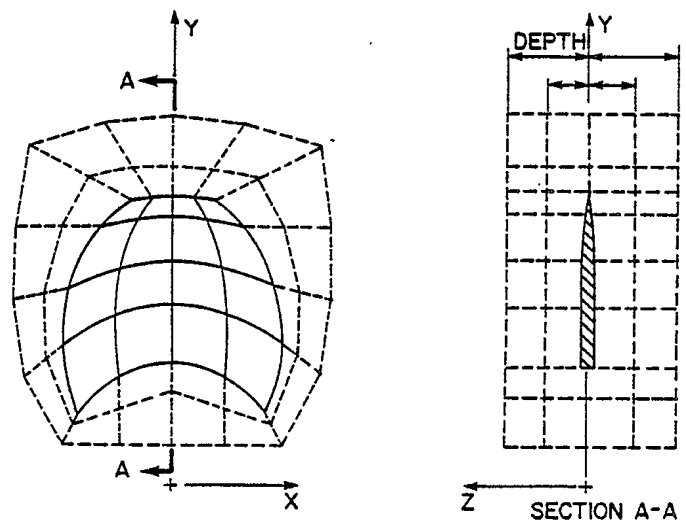


FIG.14 PLAN AND SIDE VIEWS OF DTNSRDC 4580 BLADE AND FLUID MODEL BY NORWOOD (REF.60).

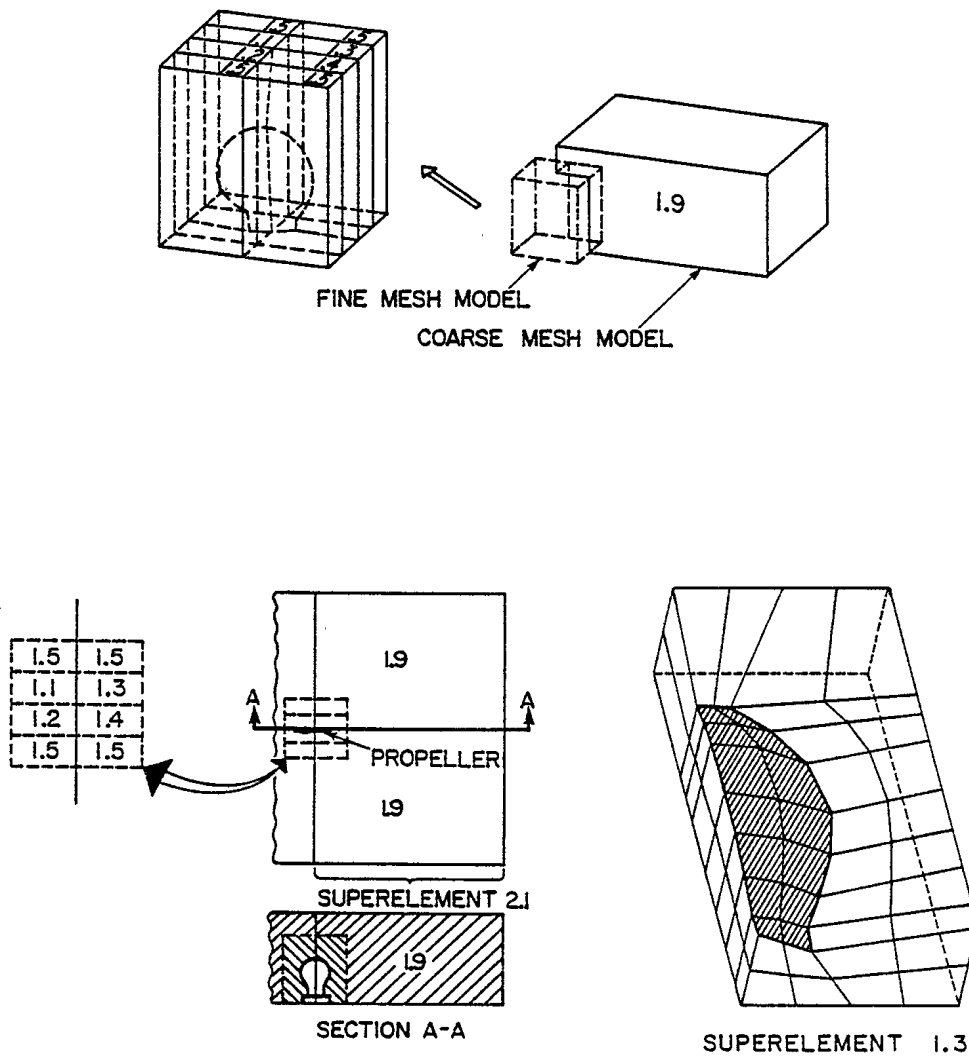
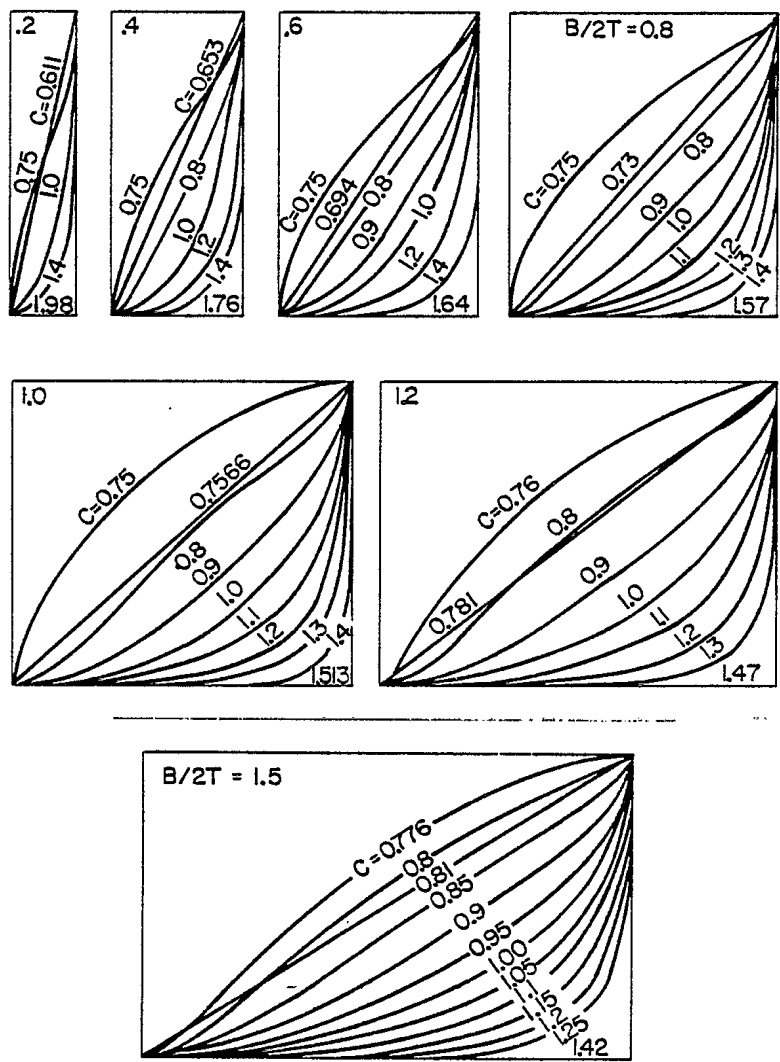


FIG.15 SUPERELEMENT MODEL OF BLADE AND FLUID BY BLAKER (REF.58).



B = BREADTH

T = DRAFT

FIG.16 TRANSFORMED SHIP HULL SECTIONS FOR ADDED MASS SECTION COEFFICIENT C BY LEWIS (REF.39).

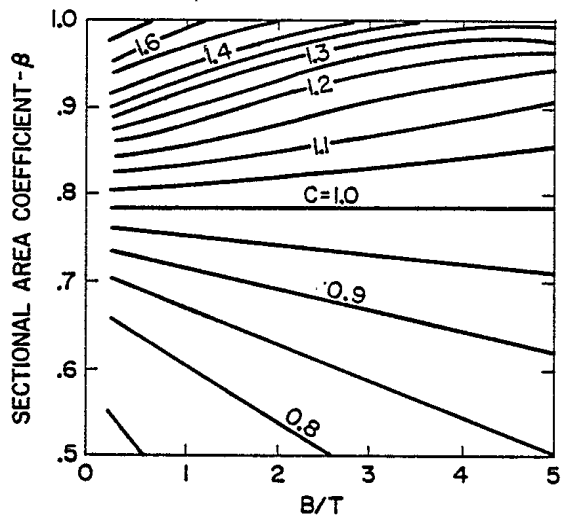


FIG.17 ADDED MASS SECTION COEFFICIENT C FROM SHIP HULL SECTIONAL AREA COEFFICIENT β BY LEWIS (REF.39).

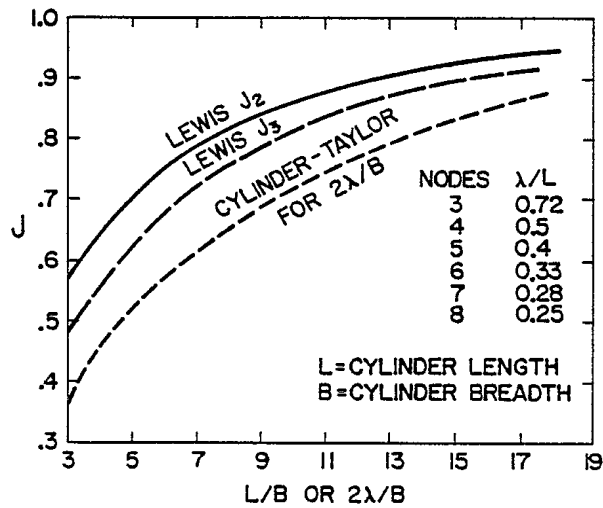


FIG.18 LONGITUDINAL REDUCTION FACTOR J FOR AN ELLIPSOID OF REVOLUTION VIBRATING Laterally WITH 2 OR 3 NODES AND A CIRCULAR CYLINDER WITH UP TO 8 NODES BY LEWIS (REF.39).

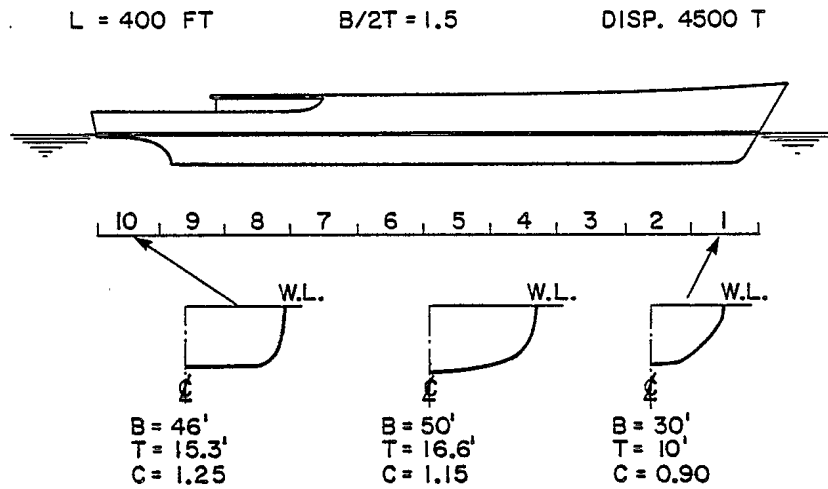


FIG.19 EXAMPLE CASE OF TYPICAL HULL FOR APPLICATION OF LEWIS' FORMULAS EQNS. (12) AND (13).

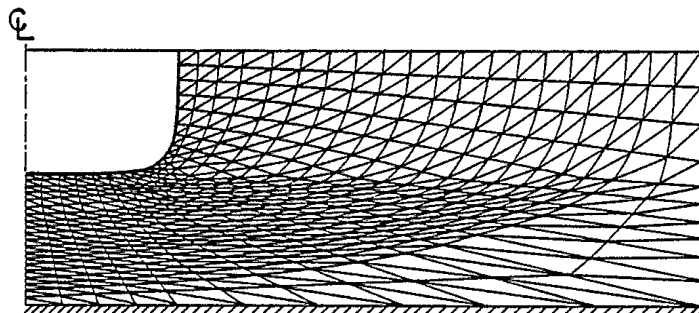


FIG.20 FINITE ELEMENT MODEL OF THE FLUID REGION AROUND A SHIP-LIKE SECTION BY MADSEN (REF.43).

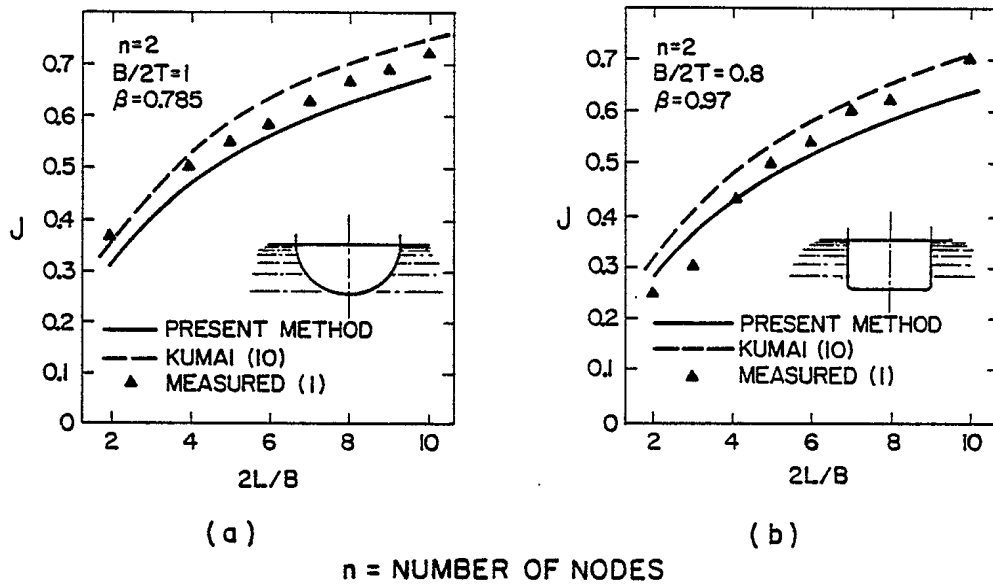


FIG. 21 J FACTOR FOR (a) CIRCULAR AND (b) RECTANGULAR SECTIONS BY MADSEN (REF. 43).

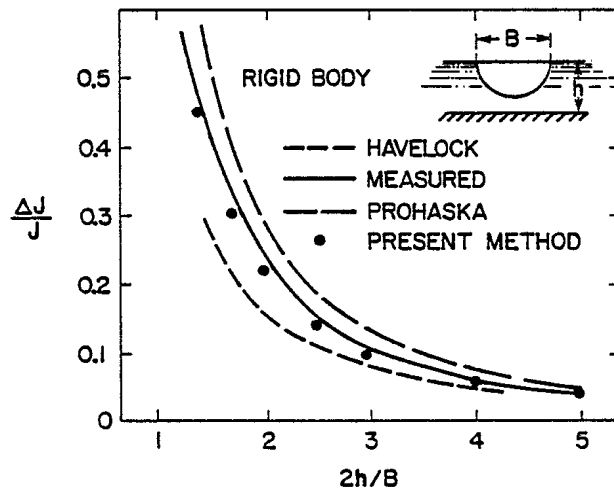


FIG. 22 CHANGE IN J DUE TO RESTRICTED WATER DEPTH (REF. 43).

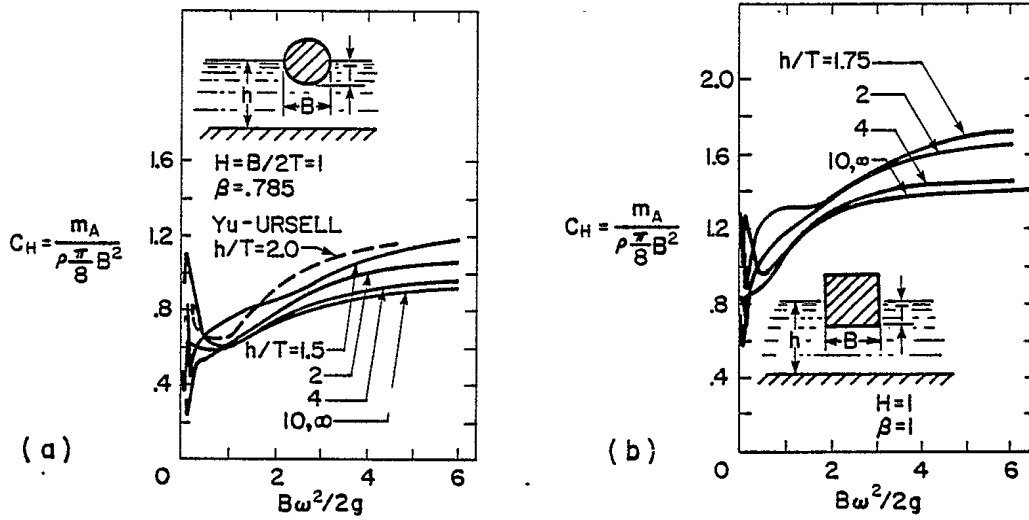


FIG. 23 HEAVE ADDED MASS COEFFICIENT C_H FOR (a) CIRCULAR AND (b) SQUARE CYLINDERS BY KIM (REF.45).

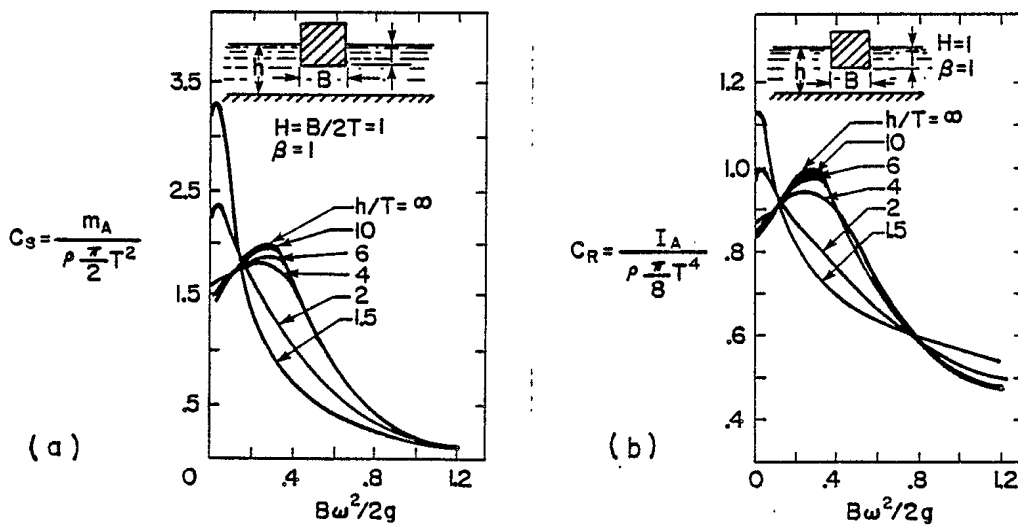


FIG. 24 (a) SWAY ADDED MASS COEFFICIENT C_S AND (b) ROLL ADDED MOMENT OF INERTIA COEFFICIENT C_R FOR SQUARE CYLINDER BY KIM (REF. 45).

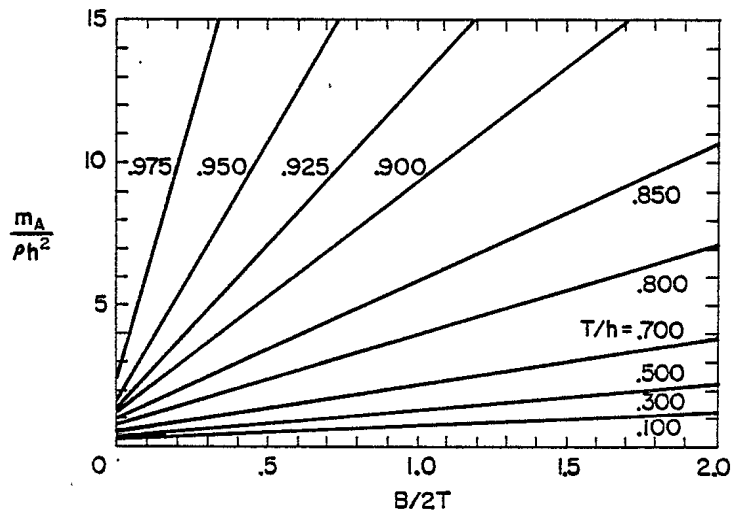


FIG.25 SWAY ADDED MASS COEFFICIENT FOR 2-D RECTANGULAR CYLINDER AT ZERO FREQUENCY BY FLAGG AND NEWMAN (REF.46).

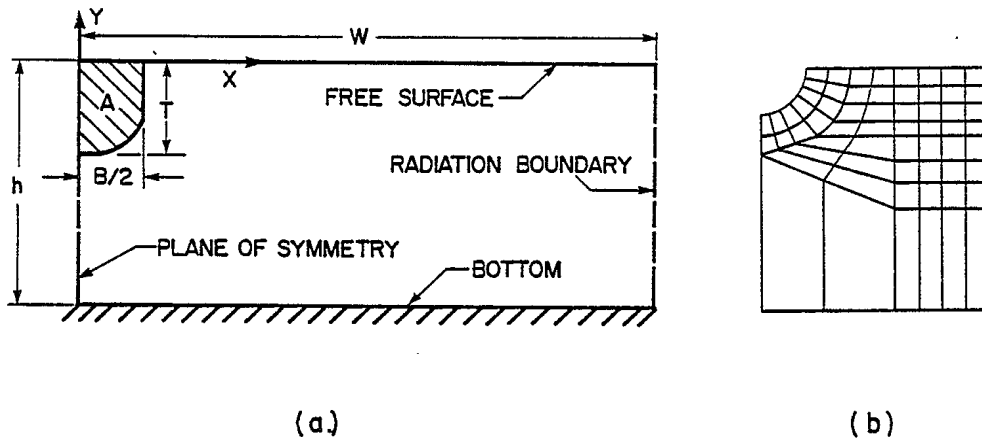


FIG. 26 (a) MODELING PARAMETERS, AND (b) GRID FOR FINITE ELEMENT ADDED MASS MODEL BY NEWTON, CHENAULT AND SMITH (REF. 51).

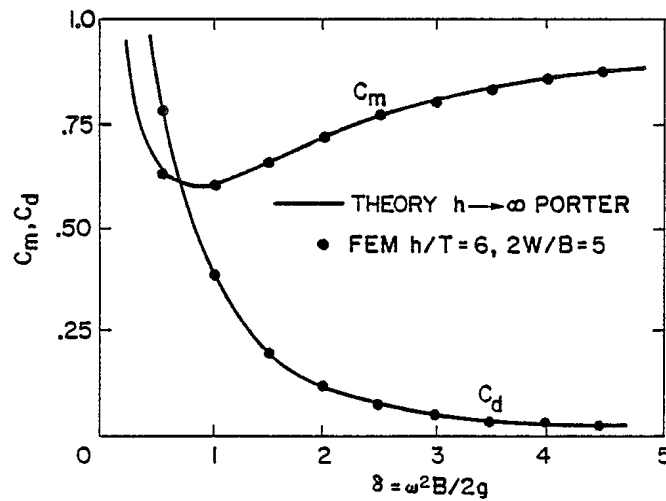


FIG. 27 HEAVE ADDED MASS AND DAMPING COEFFICIENTS C_m AND C_d FOR 2-D SEMI-CIRCULAR CYLINDER BY NEWTON, CHENAULT AND SMITH (REF. 51).

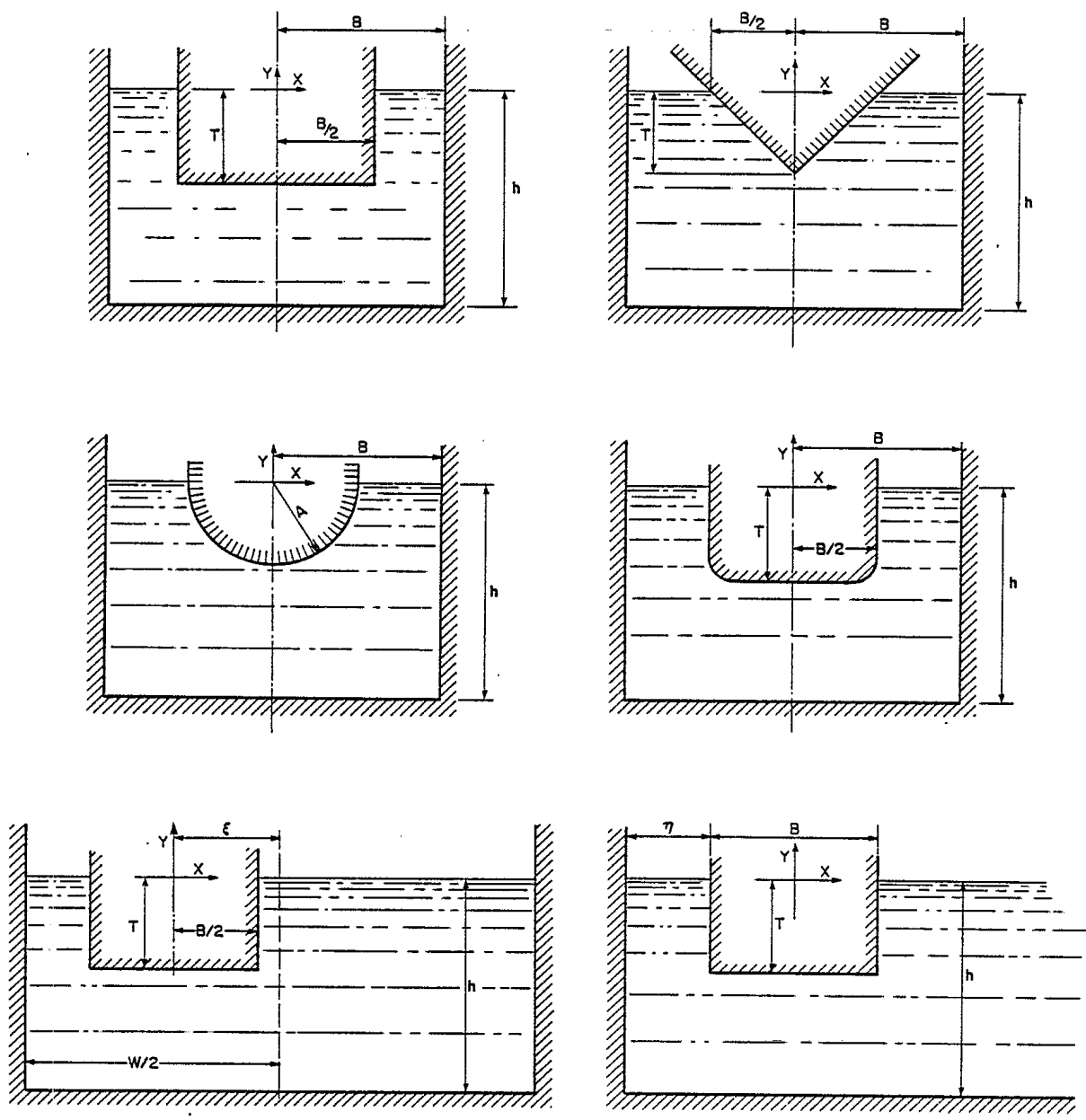


FIG.28 VARIOUS SHAPED CYLINDERS IN A CANAL FOR CALCULATION OF SWAY ADDED MASS BY BAI (REF.53).

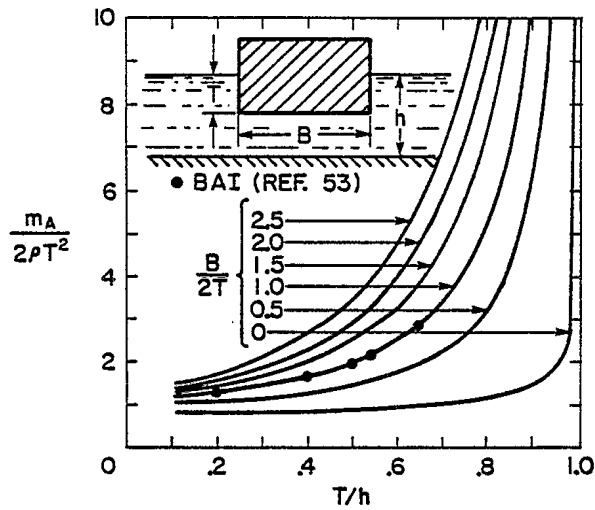
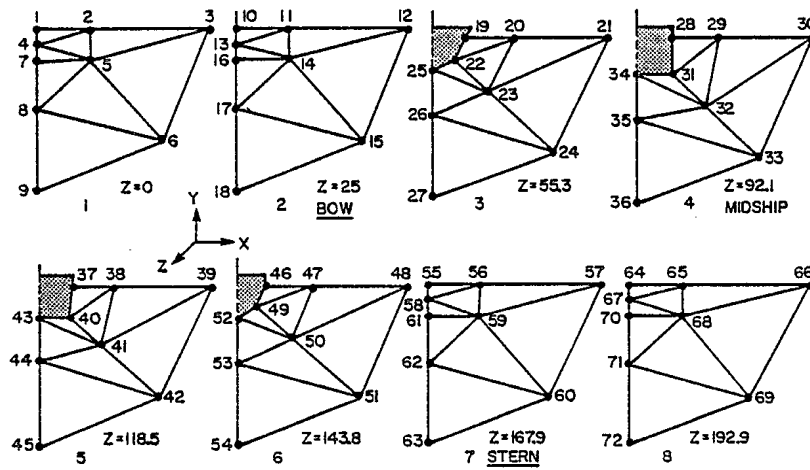


FIG.29 COMPARISON OF BAI'S RESULTS AND FLAGG AND NEWMAN'S CURVES (REF.46) FOR A RECTANGULAR CYLINDER AT ZERO FREQUENCY LIMIT.



z = DISTANCE AFT FROM FORWARD END OF FLUID MODEL IN METRES

FIG.30 FINITE ELEMENT MODEL OF FLUID SURROUNDING SHIP HULL SECTIONS BY MEIJERS (REF.55).

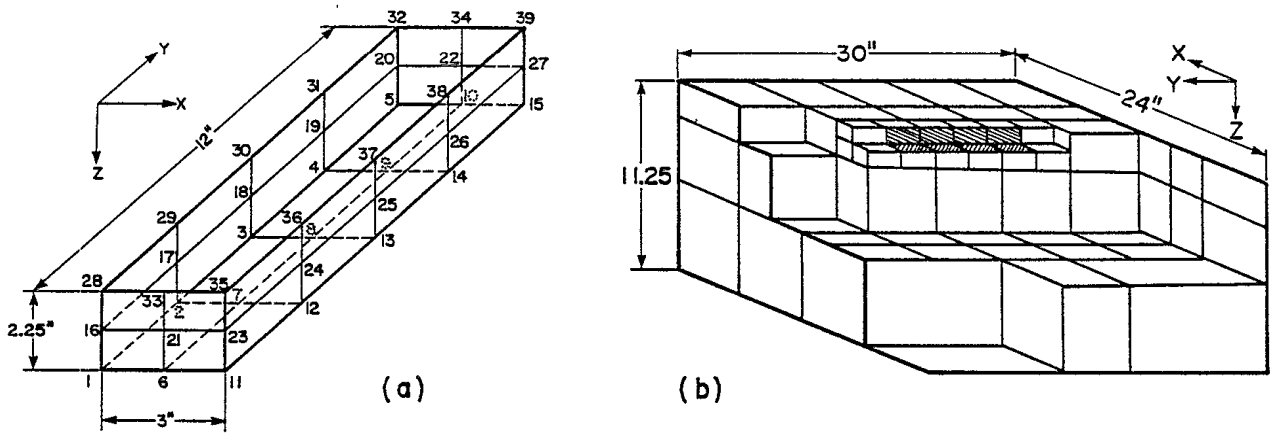


FIG.31 FINITE ELEMENT MODEL OF (a) BOX STRUCTURE AND (b) FLUID BY CHOWDHURY (REF. 56).

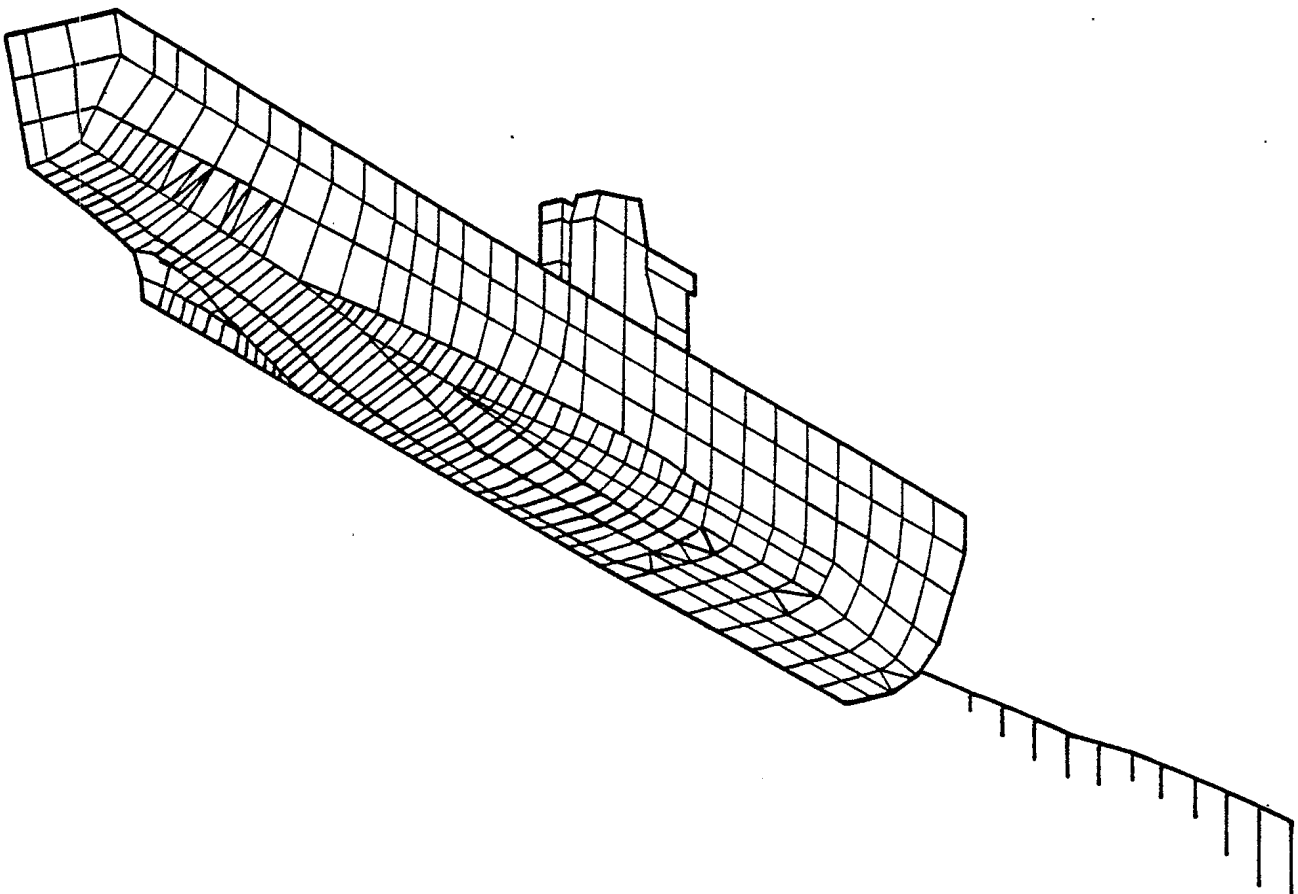


FIG.32 FINITE ELEMENT MODEL OF SHIP HULL STRUCTURE FOR PROGRAM NASTRAN BY LIEPINS AND CONAWAY (REF.75)

REFERENCES

1. Stokes, G.G., "On Some Cases of Fluid Motion", Proceedings Cambridge Philosophical Soc., Vol. 8, May 1843, pp. 105-137.
2. Lamb, H., Hydrodynamics, 6th ed., Dover, 1945, Ch. 6.
3. Rayleigh, Lord, Theory of Sound, 2nd ed., Vol. 2, Dover, 1945.
4. Geers, T.L., "Transient Response Analysis of Submerged Structures", Finite Element Analysis of Transient Nonlinear Structural Behavior, ASME, AMD-Vol. 14, 1975, pp. 59-84.
5. Kalinowski, A.J., "Fluid Structure Interaction", Shock and Vibration Computer Programs: Reviews and Summaries, Ed. by W. and B. Pilkey, U.S. Dept. of Defence, SVM-10, 1975.
6. Chen, L.H. and Pierucci, M., "Underwater Fluid-Structure Interaction Part IV: Hydrodynamically Applied Forces (Moving Medium)", The Shock and Vibration Digest, Volume 9, No. 7, July 1977, p. 29.
7. Jensen, J.J. and Madsen, N.F., "A Review of Ship Hull Vibration Part IV: Comparison of Beam Models", The Shock and Vibration Digest, Vol. 9, No. 7, July 1977, p. 13.
8. Firth, D. "Acoustic Vibration of Structures in Liquids", The Shock and Vibration Digest, Vol. 9, No. 9. Sept. 1977, p. 3.
9. Lectures on Finite Element Methods in Continuum Mechanics, NATO Advanced Study Institute, Lisbon, Sept. 1971, Ed. by J.T. Oden and E.R.A. Oliveira, University of Alabama, Huntsville, 1973.
10. Finite Element Methods in Flow Problems, International Sym. on Finite Element Methods, Swansea, Jan. 1974, Ed. by J.T. Oden, O.C. Zienkiewicz, R.H. Gallagher and C. Taylor, University of Alabama, Huntsville, 1974.
11. Shock and Vibration Computer Programs: Reviews and Summaries, Ed. by W. and B. Pilkey, The Shock and Vibration Info. Center, U.S. Dept. of Defense, NRL, Washington, D.C., 1975.
12. Structural Mechanics Computer Programs: Surveys, Assessments and Availability, Ed. by W. Pilkey, K. Saczalski and H. Schaeffer, University Press of Virginia, Charlottesville, 1974.

13. Finite Element Techniques, Proc. of the Sym. on Finite Element Techniques, Stuttgart, June 1969, Ed. by M. Sorensen, University of Stuttgart, Stuttgart, 1969.
14. Application of Computerized Methods in Analysis and Design of Ship Structures, Marine Structures, and Machinery, Symposium on Design of Marine Structures Computerized Methods, Oslo, November 1972, Det Norske Veritas, Oslo, 1972.
15. NASTRAN: Users' Experiences, Fourth NASTRAN Users' Colloquium, NASA Langley Res. Center, Hampton, Virginia, Sept. 1975, NASA TM X-3278, NASA, Washington, D.C., 1975.
16. NASTRAN: Users' Experiences, Fifth NASTRAN Users' Colloquium, NASA Ames Res. Center, Moffett Field, California, Oct. 1976, NASA TM X-3428, NASA, Washington, D.C., 1976.
17. Finite Element Methods in Engineering, Proc. of the 2nd International Conference on Finite Element Methods in Engineering, University of Adelaide, Australia, Dec. 1976, Ed. By Y.K. Cheung and S.G. Hutton, University of Adelaide, 1976.
18. Proc. of the 6th Inter. Ship Structures Congress, Boston, Aug. 1976, Vol. I and II, M.I.T., Cambridge, Mass. 1976.
19. Proc. of the 7th Inter. Ship Structures Congress, Paris, Aug, 1979, Vol. I and II, Inst. Recherche Const. Navale, Paris, France, 1979.
20. Zienkiewicz, O.C., The Finite Element Method, 3rd Ed., McGraw-Hill Book Co., London, 1977.
21. Zienkiewicz, O.C. and Newton, R.E., "Coupled Vibrations of a Structure Submerged in a Compressible Fluid", Proc. of Sym. on Finite Element Techniques, University of Stuttgart, Stuttgart, June 1969, p. 359.
22. Beranek, L.L., Acoustics, McGraw-Hill Book Co., N.Y., 1954, Ch. 5.
23. Kinsler, L.E. and Frey, A.R., Fundamentals of Acoustics, 2nd Ed., John Wiley and Sons, Inc., N.Y., 1962.
24. Imlay, F.H., "The Complete Expressions for 'Added Mass' of a Rigid Body Moving in an Ideal Fluid", NSRDC Report 1528, July 1961.

25. Birkhoff, G., Hydrodynamics, Princeton University Press, 1963.
26. Wendel, K., "Hydrodynamic Masses and Hydrodynamic Moments of Inertia", NSRDC, TMB Translation 260, July 1956.
27. Lindholm, U.S., Kana, D.D., Chu, W. and Abramson, H.N., "Elastic Vibration Characteristics of Cantilever Plates in Water", Southwest Res. Institute, Texas, Tech. Report. 1, Aug. 1962, DSIS 68/9230.
28. Lindholm, U.S., Kana, D.D., Chu, W. and Abramson, H.N., "Elastic Vibration Characteristics of Cantilever Plates in Water", J. Ship Res., Vol. 9, June 1965, p. 11.
29. Den Hartog, J.P., Mechanical Vibrations, 4th Ed., McGraw-Hill Book Co., N.Y., 1956, Ch. 7.
30. Theoredorsen, T., "General Theory of Aerodynamic Instability and the Mechanism of Flutter", NACA Report 496, 1935, DSIS 52/6838.
31. Patton. K.T. "Hydrodynamic Mass of Bodies in a Fluid", U.S. Navy, Underwater Sound Lab., T.M. 933-351-64, Oct. 1964.
32. Fritz, R.J. "The Effect of Liquids on the Dynamic Motions of Immersed Solids", Trans. ASME, J. Eng. Industry, Vol. 94, Series B, No. 1, Feb. 1972, p. 167.
33. Hagist, W.M., "Experimental Determination of the Hydrodynamic Mass of Various Bodies", University of Rhode Island, Kingston, U.S. Naval Underwater Sound Lab. Contract N70024-1024, March 1965, DSIS 65/13924.
34. Frank, W., "Oscillation of Cylinders In or Below the Free Surface of Deep Fluids", NSRDC Report 2375, Oct. 1967.
35. Frank, W., "The Heave Damping Coefficients of Bulbous Cylinders, Partially Immersed in Deep Water", J. Ship Res., Vol. 11, Sept. 1967, p. 151.
36. Bedel, J.W., "Improved Method for the Calculation of the Added Mass and Damping Coefficients of Oscillating Cylinders", NSRDC Tech. Note 216, Nov. 1971, DSIS 73/5971.
37. Landweber, L. and Macagno, M., "Added Masses of Two-Dimensional Forms by Conformal Mapping", J. Ship Res., Vol. 11, June 1967, p. 109.

38. Macagno, M., "A Comparison of Three Methods for Computing the Added Mass of Ship Sections", J. Ship Res., Vol. 12, Dec. 1968, p. 279.
39. Lewis, F.M., "Hull Vibration of Ships", Principles of Naval Architecture, Ed. by J.P. Comstock, Revised Ed., SNAME, N.Y., 1977, Ch. X.
40. Landweber, L., "Vibration of a Flexible Cylinder in a Fluid", J. Ship Res., Vol. 11, Sept. 1967, p. 143.
41. Landweber, L., "Natural Frequencies of a Body of Revolution Vibrating Transversely in a Fluid", J. Ship Res., Vol. 15, June 1971, p. 97.
42. Bishop, R.E.D., Price, W.G. and Tan, P.K.Y., "Wave-Induced Response of a Flexible Ship", Inter. Shipbldg., Vol. 24, No. 278, Oct. 1977, p. 284.
43. Madsen, N.F., "On the Influence of Three-Dimensional Effects and Restricted Water Depth on Ship Hull Vibration", Inter. Shipbuilding, Vol. 25, No. 286, June 1978, p. 151.
44. Yu, Y.S. and Ursell, F., "Surface Waves Generated by an Oscillating Circular Cylinder on Water of Finite Depth: Theory and Experiment", J. Fluid Mech., Vol. 11, 1961, p. 529.
45. Kim, C.H., "Hydrodynamic Forces and Moments for Heaving, Swaying and Rolling Cylinders on Water of Finite Depth", J. Ship Res., Vol. 13, June 1969, p. 137.
46. Flagg, C.N. and Newman, J.N., "Sway Added-Mass Coefficients for Rectangular Profiles in Shallow Water", J. Ship Res., Vol. 15, Dec. 1971, p. 257.
47. Hunt, J.T., Knittel, M.R. and Barach, D., "A Finite Element Approach to Acoustic Radiation from Elastic Structures", J. Acoust. Soc. America, Vol. 55, Feb. 1974, p. 269.
48. Kane, J.R. and McGoldrick, R.T., "Longitudinal Vibrations of Marine Propulsion - Shafting Systems", Trans. SNAME, Vol. 57, 1949, p. 193.
49. Roren, E.M.Q., "Impact of Finite Element Techniques on Practical Design of Ship Structures", Proc. of Sym. on Finite Element Techniques, Univ. of Stuttgart, Stuttgart, June 1969, p. 419.

50. Holand, I., "Finite Elements for the Computation of Hydrodynamic Mass", Proc. of Sym. on Finite Element Techniques, University of Stuttgart, Stuttgart, June 1969, p. 509.
51. Newton, R.E., Chenault, D.W. and Smith, D.A., "Finite Element Solution for Added Mass and Damping", Finite Element Methods in Flow Problems, Inter. Sym. on Finite Element Methods, Swansea, Jan. 1974, Ed. by J.T. Oden, O.C. Zienkiewicz, R.H. Gallagher and C. Taylor, University of Alabama, Huntsville, 1974, p. 159.
52. Bai, K.J., "Added Mass of a Rectangular Cylinder in a Rectangular Canal", J. Hydronautics, Vol. 11, No. 1., Jan. 1977, p. 29.
53. Bai, K.J., "Sway Added-Mass of Cylinders in a Canal Using Dual-Extremum Principles", J. Ship Res., Vol. 21, No. 4, Dec. 1977, p. 193.
54. Fujino, M., "The Effect of the Restricted Waters on the Added Mass of a Rectangular Cylinder", Eleventh Sym. on Naval Hydrodynamics, ONR, London, 1976, p. 655.
55. Meijers, P., "Natural Frequencies and Response of Three-Dimensional Elasto-Hydrodynamic Systems", Inst. TNO Report 4830/5, Delft, Jan. 1973.
56. Chowdhury, P.C., "Free Vibrations of Fluid-Borne Structures: Investigations of a Simple Model", Trans. N.E. Coast Inst. Eng and Shipbuilders, Vol. 91, No. 1, Nov. 1974, p. 15.
57. Chowdhury, P.C., "Fluid Finite Elements for Added-Mass Calculations" Inter. Shipbuilding., Vol. 19, No. 217, Sept. 1972, p. 302.
58. Blaker, B. and Krakeland, B., "Vibration of Submerged Structures as Computed by the Finite Element Method", A/S Computas Report 75-8, March 1976.
59. Norwood, M., "Application of the Finite Element Method for the Calculation of the Hydrodynamic Added Mass of Marine Propeller Blades", MARTEC Ltd., Halifax, Dec. 1977.
60. Norwood, M., "Propeller Vibration and Strength Analysis by Finite Element Methods (PVAST): User's Manual", MARTEC Ltd., Halifax, March 1983.

61. Marcus, M.S., "A Finite-Element Method Applied to the Vibration of Submerged Plates", J. Ship Res., Vol. 22, No. 2, June 1978, p. 94.
62. Everstine, G.C., Schroeder, E.A. and Marcus, M.S., "The Dynamic Analysis of Submerged Structures", Reference 15, p. 419.
63. Everstine, G.C., "A NASTRAN Implementation of the Doubly Asymptotic Approximation for Underwater Shock Response", Reference 16, p. 207.
64. Zarda, P.R., "A Finite Element-Analytical Method for Modeling a Structure in a Infinite Fluid", Reference 16, p. 251.
65. Coppolino, R.N., "A Numerically Efficient Finite Element Hydroelastic Analysis", Reference 16, p. 177.
66. Egeland, O., and Araldsen, P.O., "SESAM-69 - A General Purpose Finite Element Method Program", Computers and Structures, Pergamon Press, Great Britain, Vol. 4, 1974, p. 41. See also Ref. 14.
67. Barton, M.V., "Vibration of Rectangular and Skew Cantilever Plates", J. Applied Mech., Vol. 18, June 1951, p. 129.
68. "Vibration Analysis of a Steerable Nozzle for Heavy Duty Ship Propulsion", A/S Computas, Det Norske Veritas, Hevik, Norway, Sales Brochure.
69. Lewis, F.M. and Auslaender, J., "Virtual Inertia of Propellers", J Ship Res., Vol. 3, March 1960, p. 37.
70. Burrill, L.C. and Robson, W., "Virtual Mass and Moment of Inertia of Propellers", Trans. N.E. Coast Inst. Eng. and Shipbuilders, Vol. 78, March 1962, p. 325.
71. Norrie, D.H., "The Virtual Inertia of Propellers Under Load", J. Ship Res., Vol. 9, June 1965, p. 23.
72. Leggat, L.J. and Sponagle, N., DREA Informal Communication.
73. Altmann, R., Schaefer, K. and Bohn, J., "Non-Steady Performance Features of Semi-Submerged Supercavitating Propellers", HYDRONAUTICS Inc., Tech. Report 7307-5, Aug. 1975.

74. Paulling, J.R. and Porter, W.R., "Analysis and Measurement of Pressure and Force on Heaving Cylinders in a Free Surface", Proc. of 4th U.S. National Cong. of Applied Mechanics, ASME, University of California, Berkeley, June 1962, p. 1369.
75. Liepins, A.A. and Conaway, J.H., "Application of NASTRAN to Propeller-Induced Ship Vibration", Reference 15, p. 361.
76. Kalinowski, A.J. and Patel, J.S., "A Summary of NASTRAN Fluid/Structure Interaction Capabilities", Reference 16, p. 229.
77. Holden, K., "Vibrations of Marine Propeller Blades", Norwegian Maritime Research, Vol. 2, No. 3, 1974, pp. 2-15.
78. Norwood, M., "Hull Vibration and Strength Analysis by Finite Element Methods (HVASt): User's Manual", MARTEC LTD., Halifax, March 1982.

DOCUMENT CONTROL DATA - R & D		
(Security classification of title, body of abstract and indexing annotation must be entered when the overall document is classified)		
1. ORIGINATING ACTIVITY Defence Research Establishment Atlantic	2a. DOCUMENT SECURITY CLASSIFICATION Unclassified	
	2b. GROUP	
3. DOCUMENT TITLE A REVIEW OF HYDRODYNAMIC ADDED MASS INERTIA OF VIBRATING SUBMERGED STRUCTURES		
4. DESCRIPTIVE NOTES (Type of report and inclusive dates)		
5. AUTHOR(S) (Last name, first name, middle initial) J.E. SLATER		
6. DOCUMENT DATE APRIL 1984	7a. TOTAL NO. OF PAGES 81	7b. NO. OF REFS 78
8a. PROJECT OR GRANT NO.	9a. ORIGINATOR'S DOCUMENT NUMBER(S) DREA Technical Memorandum 84/F	
8b. CONTRACT NO.	9b. OTHER DOCUMENT NO.(S) (Any other numbers that may be assigned this document)	
10. DISTRIBUTION STATEMENT		
11. SUPPLEMENTARY NOTES	12. SPONSORING ACTIVITY	
13. ABSTRACT 50// This report is a review of the methods developed for predicting the hydrodynamic added mass inertia of vibrating structures floating or submerged in a fluid. The fluid surrounding a vibrating structure causes an apparent increase in the mass inertia of the structure, which substantially reduces the natural resonant frequencies and alters the dynamic response. The various methods consist of the three basic approaches; analytical, empirical and numerical. This report presents the merits and limitations of the methods by indicating their suitability to predict the added mass inertia effects of structures such as plates, foils, marine propellers and ship hulls. //		
<p>No one universal method has been developed to satisfactorily predict the added mass effect but a variety of methods can be used to handle many configurations of interest. For detailed analysis, the numerical finite element methods are vastly superior. Nonetheless, for conceptual and preliminary design analyses, simpler methods using analytical and empirical formulas may be sufficiently accurate besides being faster and cheaper to use than finite element modeling of the fluid. However, some of these methods are applicable only to 2-D or axisymmetric structures as well as being restricted to essentially the zero frequency limit.</p>		

KEY WORDS

Hydrodynamic Mass
 Added Mass Inertia
 apparent mass
 virtual mass
 water entrainment
 Fluid-structure interaction
 Vibrating Submerged Structures
 Plates in water
 Marine propellers
 Ship hull added mass
 Fluid Finite Element

INSTRUCTIONS

1. **ORIGINATING ACTIVITY:** Enter the name and address of the organization issuing the document.
- 2a. **DOCUMENT SECURITY CLASSIFICATION:** Enter the overall security classification of the document including special warning terms whenever applicable.
- 2b. **GROUP:** Enter security reclassification group number. The three groups are defined in Appendix 'M' of the DRB Security Regulations.
3. **DOCUMENT TITLE:** Enter the complete document title in all capital letters. Titles in all cases should be unclassified. If a sufficiently descriptive title cannot be selected without classification, show title classification with the usual one-capital-letter abbreviation in parentheses immediately following the title.
4. **DESCRIPTIVE NOTES:** Enter the category of document, e.g. technical report, technical note or technical letter. If appropriate, enter the type of document, e.g. interim, progress, summary, annual or final. Give the inclusive dates when a specific reporting period is covered.
5. **AUTHOR(S):** Enter the name(s) of author(s) as shown on or in the document. Enter last name, first name, middle initial. If military, show rank. The name of the principal author is an absolute minimum requirement.
6. **DOCUMENT DATE:** Enter the date (month, year) of Establishment approval for publication of the document.
- 7a. **TOTAL NUMBER OF PAGES:** The total page count should follow normal pagination procedures, i.e., enter the number of pages containing information.
- 7b. **NUMBER OF REFERENCES:** Enter the total number of references cited in the document.
- 8a. **PROJECT OR GRANT NUMBER:** If appropriate, enter the applicable research and development project or grant number under which the document was written.
- 8b. **CONTRACT NUMBER:** If appropriate, enter the applicable number under which the document was written.
- 9a. **ORIGINATOR'S DOCUMENT NUMBER(S):** Enter the official document number by which the document will be identified and controlled by the originating activity. This number must be unique to this document.
- 9b. **OTHER DOCUMENT NUMBER(S):** If the document has been assigned any other document numbers (either by the originator or by the sponsor), also enter this number(s).
10. **DISTRIBUTION STATEMENT:** Enter any limitations on further dissemination of the document, other than those imposed by security classification, using standard statements such as:
 - (1) "Qualified requesters may obtain copies of this document from their defence documentation center."
 - (2) "Announcement and dissemination of this document is not authorized without prior approval from originating activity."
11. **SUPPLEMENTARY NOTES:** Use for additional explanatory notes.
12. **SPONSORING ACTIVITY:** Enter the name of the departmental project office or laboratory sponsoring the research and development. Include address.
13. **ABSTRACT:** Enter an abstract giving a brief and factual summary of the document, even though it may also appear elsewhere in the body of the document itself. It is highly desirable that the abstract of classified documents be unclassified. Each paragraph of the abstract shall end with an indication of the security classification of the information in the paragraph (unless the document itself is unclassified) represented as (TS), (S), (C), (R), or (U).

The length of the abstract should be limited to 20 single-spaced standard typewritten lines; 7/8 inches long.
14. **KEY WORDS:** Key words are technically meaningful terms or short phrases that characterize a document and could be helpful in cataloging the document. Key words should be selected so that no security classification is required. Identifiers, such as equipment model designation, trade name, military project code name, geographic location, may be used as key words but will be followed by an indication of technical context.

121964
 84-02593